ERDC TR-15-2

Engineer Research and Development Center

US Army Corps of Engineers®
Engineer Research and Development Center

ERDC
INNOVATIVE SOLUTIONS for a safer, better world

Engineering for Polar Operations, Logistics, and Research (EPOLAR)

High-Performance Plastic Sled Design for Polar Traversing

Jason C. Weale, James H. Lever, and Jonathan Trovillion

June 2015

High-Performance Plastic Sled Design for Polar Traversing

Jason C. Weale and James H. Lever

Cold Regions Research and Engineering Laboratory (CRREL)
U.S. Army Engineer Research and Development Center (ERDC)
72 Lyme Road
Hanover, NH 03755-1290

Jonathan Trovillion

Construction Engineering Research Laboratory (CERL)
U.S. Army Engineer Research and Development Center (ERDC)
2902 Newmark Drive
Champaign, IL 61822-9005

Final Report

Prepared for National Science Foundation, Division of Polar Programs
Arlington, VA 22230

Under Engineering for Polar Operations, Logistics, and Research (EPOLAR)
EP-ANT-11-05, "Field Support for SPoT";
EP-ANT-12-16, "High-Performance Polar Sleds";
EP-ANT-13-46, "Models and Materials for SPoT Cargo and Fuel Sleds";
EP-ARC-10-12, "Field Support for GrIT"; and
EP-ARC-12-12, "Field Support for GrIT"

Abstract

Over-snow resupply traverses in Antarctica and Greenland tow high-efficiency fuel sleds that consist of flexible fuel bladders strapped to flexible sheets of high molecular weight polyethylene (HMW-PE). Despite low towing stresses, initial HMW-PE sheets were prone to cracking and failure within 1 to 2 years of service. This report describes the results of low-temperature, uniaxial tensile tests, following ASTM Standard D638, that we used to set specifications on HMW-PE sheets for polar sleds, aiming to increase service life. Tests of the original HMW-PE formulations showed significant reductions in ductility, as measured by percent elongation at break, at −40°C compared with 23°C. HMW-PE manufacturers subsequently cooperated to supply sheets with greater low-temperature ductility, and the rate of sled breakages decreased dramatically. Performance specifications for new HMW-PE sheets for polar traverses now include a requirement for greater than 60% elongation at break at −40°C, as measured using ASTM 638 uniaxial tensile tests.

Contents

Illustrations

Figures

Tables

Preface

These tests were conducted for the National Science Foundation, Division of Polar Programs (NSF-PLR) under Engineering for Polar Operations, Logistics, and Research (EPOLAR) EP-ANT-11-05, "Field Support for SPoT"; EP-ANT-12-16, "High-Performance Polar Sleds"; EP-ANT-13-46, "Models and Materials for SPoT Cargo and Fuel Sleds"; EP-ARC-10-12, "Field Support for GrIT"; and EP-ARC-12-12, "Field Support for GrIT." The technical monitors were George Blaisdell, Chief Program Manager, NSF-PLR, U.S. Antarctic Program (USAP), and Pat Haggerty, Program Manager, NSF-PLR, Arctic Sciences (ARC).

The work was performed by Jason C. Weale and Dr. James H. Lever (Force Projection and Sustainment Branch, Dr. Edel Cortez, Chief) of the U.S. Army Engineer Research and Development Center, Cold Regions Research and Engineering Laboratory (ERDC-CRREL), and Jonathan C. Trovillion of the U.S. Army Engineer Research and Development Center, Construction Engineering Research Laboratory (ERDC-CERL). At the time of publication, Janet Hardy was the program manager for EPOLAR. Dr. Loren Wehmeyer was Chief of the Research and Engineering Division of ERDC-CRREL. The Deputy Director of ERDC-CRREL was Dr. Lance Hansen, and the Director was Dr. Robert Davis.

The authors thank Glenn Durell of ERDC-CRREL for his technical expertise in using and adapting the equipment to perform these tests. They sincerely thank George Blaisdell at NSF-PLR-USAP and Pat Haggerty and Renee Crain at NSF-PLR-ARC for their enthusiastic support of the South Pole Traverse (SPoT) and the Greenland Inland Traverse (GrIT).

LTC John T. Tucker III was Commander of ERDC; and Dr. Jeffery P. Holland was the Director.

Acronyms and Abbreviations

AFS	Vendor A Field Sample
AR1	Vendor A Revision 1
AR2	Vendor A Revision 2
ARC	Arctic Sciences
ASTM	American Society for Testing and Materials
BFS	Vendor B Field Sample
BR1	Vendor B Revision 1
BR2	Vendor B Revision 2
CERL	U.S. Army Construction Engineering Research Laboratory
COTS	Commercial Off the Shelf
CRREL	U.S. Army Cold Regions Research and Engineering Laboratory
EAB	Elongation at Break
EPOLAR	Engineering for Polar Operations, Logistics and Research
ERDC	Engineer Research and Development Center
FS	Field Sample
GrIT	Greenland Inland Traverse
HMW-PE	High Molecular Weight Polyethylene
LVDT	Linear Variable Differential Transformer
MTM	Material Testing Machine
NSF	National Science Foundation
PLR	Division of Polar Programs
SPoT	South Pole Traverse
USAP	U.S. Antarctic Program
UV	Ultraviolet

Unit Conversion Factors

Multiply	By	To Obtain
cubic feet	0.02831685	cubic meters
cubic inches	1.6387064 E-05	cubic meters
degrees Fahrenheit	(F-32)/1.8	degrees Celsius
feet	0.3048	meters
foot-pounds force	1.355818	joules
gallons (U.S. liquid)	3.785412 E-03	cubic meters
inches	0.0254	meters
miles (U.S. statute)	1,609.347	meters
miles per hour	0.44704	meters per second
pounds (force)	4.448222	newtons
pounds (force) per square inch	6.894757	kilopascals
pounds (mass)	0.45359237	kilograms
pounds (mass) per cubic foot	16.01846	kilograms per cubic meter
pounds (mass) per cubic inch	2.757990 E+04	kilograms per cubic meter
square feet	0.09290304	square meters
square inches	6.4516 E-04	square meters

1 Introduction

The National Science Foundation, Division of Polar Programs (NSF-PLR), operates over-snow traverses in Antarctica and Greenland to resupply their science stations. The 1030-mile (one way) South Pole Traverse (SPoT) begins at McMurdo Station on Ross Island, travels across the Ross Ice Shelf, up the Leverett Glacier, and then over the Polar Plateau to South Pole Station. The 730-mile (one way) Greenland Inland Traverse (GrIT) begins at Thule Air Base, climbs an undulating transition, and then continues on to Summit Station along the main ice sheet. Both of these environments are high latitude, high elevation, and cold.

These traverses have come to rely on high molecular weight polyethylene (HMW-PE) sheets for towing large quantities of fuel in an extremely efficient manner (Lever and Weale 2012). The HMW-PE sheets measure 8 ft wide × 68 ft long × 0.5 in. thick. Flexible fuel bladders are strapped to the sheets, which are towed through bolted steel plates at the front. The availability of long, extruded sheets of HMW-PE allows two 3000 gal. fuel bladders to be towed inline on each sled (Figure 1). A single traverse tractor can typically tow between four and six such sleds (eight and twelve bladders, respectively) over natural polar snow. These "bladder sleds" have a lower tare weight and towing resistance (i.e., they require much less tractor drawbar per unit payload towed) and are lower cost than comparable steel tank sleds. They have led to a large payback for SPoT (Lever and Thur 2014).

Figure 1. Fuel sleds towed outbound from McMurdo Station to South Pole Station in 2010–11. Each 8 ft wide × 68 ft long × 0.5 in. thick HMW-PE sheet carries two 3000 gal. fuel bladders.

Despite material-property specifications that appeared to be adequate for our needs, some HMW-PE sheets failed catastrophically during early in-field service (Figure 2). These failures were not typically located near the fronts of the sleds, where towing forces are highest. Also, they appeared to be brittle failures (sharp cracks with little ductile necking) despite manufacturer's data that suggest the material is extremely ductile and low-temperature tolerant.

Figure 2. A crack in HMW-PE sheet during outbound trip to South Pole in 2010–11.

Bladder sleds in Antarctica and Greenland initially used white HMW-PE sheets. These sheets failed at an unacceptably high rate during their first two seasons of use. At our recommendation, both traverses switched to black HMW-PE to improve ultraviolet (UV) resistance. Nevertheless, in-service failures continued to occur.

To help understand the causes of these failures, we conducted tensile tests of black HMW-PE samples supplied to SPoT and GrIT. We followed American Society for Testing and Materials Standard ASTM D638, *Standard Test Method for Tensile Properties of Plastics* (ASTM 2010), using latitude in the standard to conduct tests at the low temperatures and high deformation rates that the sleds must survive in Antarctica and Greenland. We then set performance specifications based on the results of these tests and the corresponding HMW-PE in-service failure rates. All subsequent HMW-PE sheet procurements for Antarctic and Greenland traverses have used these performance specifications.

This report is organized chronologically. It first presents results of our initial series of tensile tests conducted on commercial off-the-shelf (COTS) HMW-PE samples manufactured by three different vendors and discusses these findings. It then describes our efforts to establish minimum performance specifications and to encourage manufacturers to revise their HMW-PE plastic mixes to improve field performance. Because in-service sheet failures have been brittle fractures, we focused on improving HMW-PE ductility, characterized by average elongation at break (EAB) for specimens tested in low-temperature tensile tests. We tested samples of revised HMW-PE material from two manufacturers. These consisted of new, unused material supplied to SPoT and GrIT and samples from in-service sheets after various periods of field use. Insofar as possible, we have correlated measured EAB values with subsequent in-service failure rates. All tests were conducted at the U.S. Army Cold Regions Research and Engineering Laboratory (CRREL).

2 Service Conditions and Performance Requirements

Although SPoT's route is longer than GrIT's, both traverses encounter combinations of severe weather, low temperatures, and spatially varied snow strength and roughness. The impacts of catastrophic sheet failures are severe for both traverses: replacement cost, lost time, and risk of fuel spill through fuel-bladder damage. Consequently, the environmental, operational, and performance requirements for their HMW-PE sheets are very similar.

The HMW-PE sheets must operate at temperatures as low as −40°C and be unaffected by storage at temperatures of approximately −55°C. They must endure long-term tensile stresses of 200 psi from towing forces and behave elastically while traversing 2–5 ft high surface features known as sastrugi. These features are wind-sculpted, consist primarily of strong snow, and can have fairly sharp crests (radii of just a few inches). The crests can also be three-dimensional, providing multi-axial, concentrated loads under the sleds. Additionally, the high latitudes, high elevations (about 10,000 ft), and 24 hr summer daylight create significant UV exposure.

When designing the bladder sleds, our investigations into the material properties of HMW-PE indicated that several vendors produced similar products. Appendix A lists the material-property specifications for Vendor A, Vendor B, and Vendor C COTS materials. These properties appeared to meet our needs. In particular, peak towing forces produce tensile stresses in the HMW-PE sheets that are less than 10% of the reported tensile strength at yield (3600 psi). The large EAB specified by each vendor (greater than 600%) suggested highly ductile behavior if stresses caused local yielding, for example while bending over sastrugi. Although these specifications were for room temperature, the stated "brittleness temperature" of −90°C, −118°C, and −75°C, respectively, for Vendors A, B, and C gave some expectation of acceptable performance at −40°C.

In addition to meeting environmental and operating conditions along both traverse routes, we expect the HMW-PE sheets to achieve a minimum service life of 7 years at a rate of one round-trip to South Pole each year. Ideally, the service replacement life would extend to 10 years and thus meet the replacement life cycle of the traverse tractors. In either case, it is essential to field a reliable product where we understand and can predict the replacement life cycle to minimize random and potentially catastrophic field failures.

3 Selection of a Standard Test and Initial Specimens

High loading rates and low temperatures both act to reduce ductility of HMW-PE and thereby increase the likelihood of brittle failure. We clearly needed to understand this effect and to quantify material properties at loading rates and temperatures that reflected service conditions.

We chose to conduct a set of tests that adhered to ASTM D638, *Standard Test Method for Tensile Properties of Plastics* (ASTM 2010). This uniaxial tension test forms the basis for several important material properties of HMW-PE included in manufacturers' specification sheets (tensile strength at yield, tensile strength at break, and EAB). It is relatively easy to implement, and CRREL possesses a computer-controlled material-testing apparatus with an environmental enclosure to allow precise control of the deformation rate (crosshead speed) and temperature. In addition, HMW-PE sheets that failed in the field showed virtually no elongation or yield prior to breaking (no "necking" of plastic), which suggests brittle failure due to low temperature, high strain rate, or a combination of both. Tensile tests offer a reasonable way to reveal this effect.

To reflect service conditions, ASTM (2010) D638 provides latitude for varying both the crosshead speed and test temperature from those specified in the standard. Section 4.2 of the standard, however, notes that

> [t]ensile properties may vary with specimen preparation and with speed and environment of testing. Consequently, where precise comparative results are desired, these factors must be carefully controlled.

Our material-testing apparatus can control specific test conditions quite well. To reveal the consequence of these conditions, we developed a test matrix that would "sweep" both temperature (23°C to −40°C) and crosshead rate (20 to 80 in./min) across a range of conditions that the sleds could experience in the field. We defined the intersection of these two sweeps (−40°C, 20 in./min) as our "required field-service condition." Note that 23°C and 20 in./min are conditions explicitly listed in ASTM (2010) D638, and we included these as a baseline although the temperature is much higher than the service range for polar traverses. To control specimen preparation variability, the same individual prepared all samples and used the same equipment in the CRREL machine shop.

We obtained, on request, samples of new, unused, black, 0.5 in. thick HMW-PE from Vendors A and B, from which we prepared the majority of specimens for testing. Vendor A representatives have stated that their black HMW-PE sheets contain 1% by mass carbon black and that the strength properties of their black and white HMW-PE are identical. They also stated that the HMW-PE samples we received were from the production run that supplied black sheets for SPoT in 2010. Vendor B representatives have stated that their black HMW-PE sheets contain 2%–2.5% by mass carbon black. They also stated that the HMW-PE samples were from the production run that supplied black sheets for SPoT in 2009.

In addition, we obtained a sample of a Vendor A black HMW-PE sheet that failed during its first year of service (2010) as a bladder sled on SPoT10-11. Three of the 24 sheets from this procurement failed during SPoT10-11's outbound trip to South Pole. We obtained a sample of one of the four Vendor B black HMW-PE sheets that survived two years of service (2009–11) on SPoT09-10 and SPoT10-11. We tested specimens from these samples at our required field-service conditions to identify any changes in material properties potentially caused by field use.

4 Tensile Test Description

We performed uniaxial tensile tests in a temperature-controlled test chamber on a closed-loop, electro-hydraulic, material-testing machine (MTM). It has a 25,000 lb actuator with a 6 in. stroke. A linear variable differential transformer (LVDT) incorporated in the actuator controlled the crosshead rate and measured total deformation. A clip-on extensometer to measure axial extension was mounted in the narrow section of the specimen and had a total range of 0.5 in. over a 2 in. gage length. A 25,000 lb load cell mounted in line with the test fixture measured tensile force. Instrument tolerances and calibration dates were as follows: load cell ±0.22%, December 2010; LVDT ±0.64%, December 2010; and extensometer ±0.4%, April 2011.

The MTM controller was programmed for the desired constant crosshead rate. The controller also acquired time series load-cell, LVDT, extensometer, and temperature data. Manual vise-type grips with serrated jaws held the samples. The grips were rated at 4500 lb.

The insulated test chamber measures 20 in. wide, 36 in. deep, and 40 in. high. A cascade refrigeration system circulated cold air, using a thermocouple in the exiting air stream as feedback to control chamber temperature (±0.1°C). The chamber is capable of reaching and maintaining −70°C. Figure 3 shows a HMW-PE specimen ready for testing.

According to ASTM (2010) D638, nominal material thickness of 0.5 in. requires use of “Type III” specimens machined to a “dog bone” shape (Figure 4) with dimensions specified in Table 1. The standard requires at least five replicate tests at each set of conditions. It also requires measurement and reporting of dimensions of the actual specimens. Appendix B includes these measurements.

Figure 3. HMW-PE specimen ready for tensile testing inside environmental chamber.

Figure 4. HMW-PE specimen shape (after ASTM 2010) with dimensions given in Table 1.

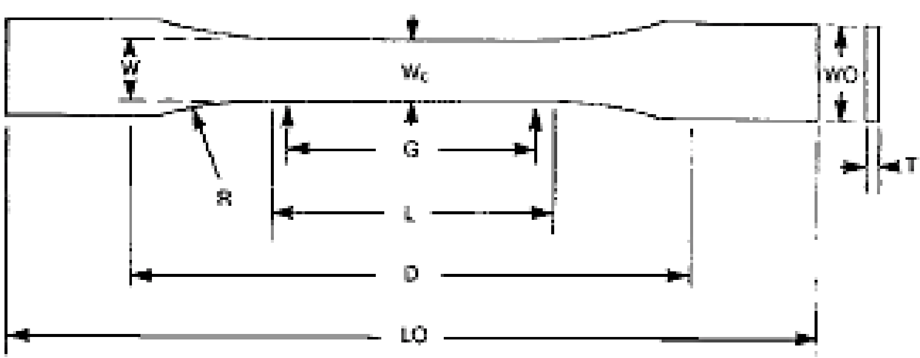

Table 1. Required dimensions (in.) for specimen of thickness *T* = 0.5 in. (per ASTM 2010).

Type III Specimen Dimensions for a Sample between 0.28 and 0.55 in. thick (reference Figure 4)	
W—Width of narrow section	0.75
L—Length of narrow section	2.25
WO—Width overall (nominal minimum)	1.13
LO—Length overall (nominal minimum)	9.7
G—Gage length	2.00
D—Distance between grips	4.5
R—Radius of fillet	3.00

As noted, we selected our baseline condition as 23°C and 20 in./min crosshead speed. Over a 2 in. gage length, this corresponds to 10 in./in./min nominal strain rate. These conditions are included in ASTM (2010) D638 for testing Type III specimens. However, service temperatures for HMW-PE bladder sleds are less than 0°C, and our concern is with temperatures as low as −40°C. Consequently, we selected −20°C and −40°C as the two other test temperatures. We held the crosshead rate at 20 in./min to sweep through these temperatures in the test matrix.

Calculations suggested that bending of an HMW-PE sheet as a bladder sled traverses sastrugi would likely generate the highest tensile stresses in service. A one-dimensional analysis (Appendix C) allowed us to estimate strain rate or crosshead rate for this case. For a 0.5 in. thick sheet conforming to a 10 in. radius crest at 5 mph (nominal traverse speed), strain rate in the outer fibers would be about 0.25/s. The corresponding crosshead rate for the test specimens would be about 34 in./min. This is relatively close to the standard 20 in./min; and we selected 40 and 80 in./min to examine the effect of higher deformation rates on HMW-PE behavior, holding test temperature at −40°C. As noted, on completion of testing using new, unused samples, we conducted tests at −40°C and 20 in./min using specimens made from a sheet of Vendor A black HMW-PE that failed during its first year in service for SPoT and using specimens made from a sheet of Vendor B black HMW-PE that survived two years of service for SPoT. Tables 2 and 3 present the test matrixes for Vendor A and Vendor B HMW-PE samples, respectively.

Table 2. Vendor A tensile-test matrix. AFS.1 specimens were made from an HMW-PE sheet that failed during its first year of service. All other specimens were made from new, unused HMW-PE from the same production run as sheets supplied to SPoT. For equipment-testing purposes, one room-temperature (A.1) specimen was destroyed during setup.

Test Series	Temp (°C)	Crosshead Rate (in./min)	# Specimens	Specimen ID	Data Rate (Hz)
A.1	Room (23)	20	4	A21–A24	200
A.2	−20	20	5	A1–A5	200
A.3	−40	20	5	A6–A10	200
A.4	−40	40	5	A11–A15	400
A.5	−40	80	5	A16–A20	800
AFS.1	−40	20	6	AFS1–AFS6	200

Table 3. Vendor B tensile-test matrix. BFS.1 specimens were made from an HMW-PE sheet that survived two years of service for SPoT. All other specimens were made from new, unused HMW-PE from the same production run as sheets supplied to SPoT.

Test Series	Temp (°C)	Crosshead Rate (in./min)	# Specimens	Specimen ID	Data Rate (Hz)
B.1	Room (23)	20	5	B21–B25	200
B.2	−20	20	5	B1–B5	200
B.3	−40	20	5	B6–B10	200
B.4	−40	40	5	B11–B15	400
B.5	−40	80	5	B16–B20	800
BFS.1	−40	20	6	BFS1–BFS6	200

5 Original Investigations: Test Results

The new, unused specimen tests were conducted on 22 and 23 March 2011, and the field-service specimen tests were conducted on 14 April 2011. Appendix D includes a comprehensive summary of the test results for all individual samples. Tables 4 (Vendor A) and 5 (Vendor B) summarize the results for each test series.

ASTM (2010) D638 provides definitions for various test results. Figures 5 and 6 show force-displacement and stress-strain plots characteristic of Vendor A and Vendor B HMW-PE specimens, respectively, to illustrate application of these definitions.

Tensile stress is load per unit area of the minimum original cross section, and strain is the increase in length measured in the gage length divided by the original gage length. The yield point is the first point on the stress-strain curve at which an increase in strain occurs without an increase in stress. The stress at this point is the tensile stress at yield, or yield stress. For all specimens tested, the yield stress was also the maximum stress. After the yield point, all specimens showed reduced stress with increasing strain until they ruptured. Thus, the tensile stress at break was always lower than the yield stress.

As seen in Figures 5 and 6, specimens displayed very little “toe” behavior (displacement at the onset of loading), indicating that the grips seated well and that there was not any play in the system. Furthermore, the stress-strain plots all displayed reasonably linear behavior for small strain; and we used linear best-fit lines between 0.0015 to 0.01 strain, based on extensometer data, to calculate Young’s modulus. Appendix E shows representative curves for a field specimen tested at −40°C and 20 in./min.

Table 4. Summary of results for each Vendor A test series. Note that we excluded the results from one specimen from field series AFS.1 owing to brittle failure at the yield point. ("FS" denotes "field sample.")

Test Series		Tensile Stress at Yield (psi)	Tensile Stress at Break (psi)	Elongation at Break (%)	Young's Modulus (psi)
A.1	avg.	4320	2140	95.8	177,770
	st. dev.	30	60	1.05	3250
A.2	avg.	6260	3250	41.6	328,540
	st. dev.	40	120	1.87	4690
A.3	avg.	7440	3820	31.1	410,630
	st. dev.	170	120	1.77	26,160
A.4	avg.	7550	4060	32.4	406,470
	st. dev.	40	210	5.07	6270
A.5	avg.	7670	4000	33.2	405,650
	st. dev.	90	160	2.29	7910
AFS.1	avg.	7240	3440	35.8	389,860
	st. dev.	40	290	0.93	8260

Table 5. Summary of results for each Vendor B test series. Note that we excluded the results at break from one room-temperature specimen (series B.1) because it did not break at a full 6 in. elongation.

Test Series		Tensile Stress at Yield (psi)	Tensile Stress at Break (psi)	Elongation at Break (%)	Young's Modulus (psi)
B.1	avg.	4200	2610	188.9	186,200
	st. dev.	30	80	40.3	3500
B.2	avg.	6150	3500	73.3	337,100
	st. dev.	20	140	6.3	6500
B.3	avg.	7360	4090	53.5	401,700
	st. dev.	70	120	3.5	7,700
B.4	avg.	7520	4120	48.8	439,100
	st. dev.	50	180	2.8	15,500
B.5	avg.	7660	4070	49.2	420,800
	st. dev.	60	310	4.2	9500
BFS.1	avg.	7280	2900	35.6	414,800
	st. dev.	50	1020	4.6	10,300

Figure 5. Typical force-displacement plot (*upper*) and stress-strain plot (*lower*) for Vendor A HMW-PE specimens (specimen A-22: 23°C and 20 in./min). Tensile stress at yield was the maximum stress for all test specimens.

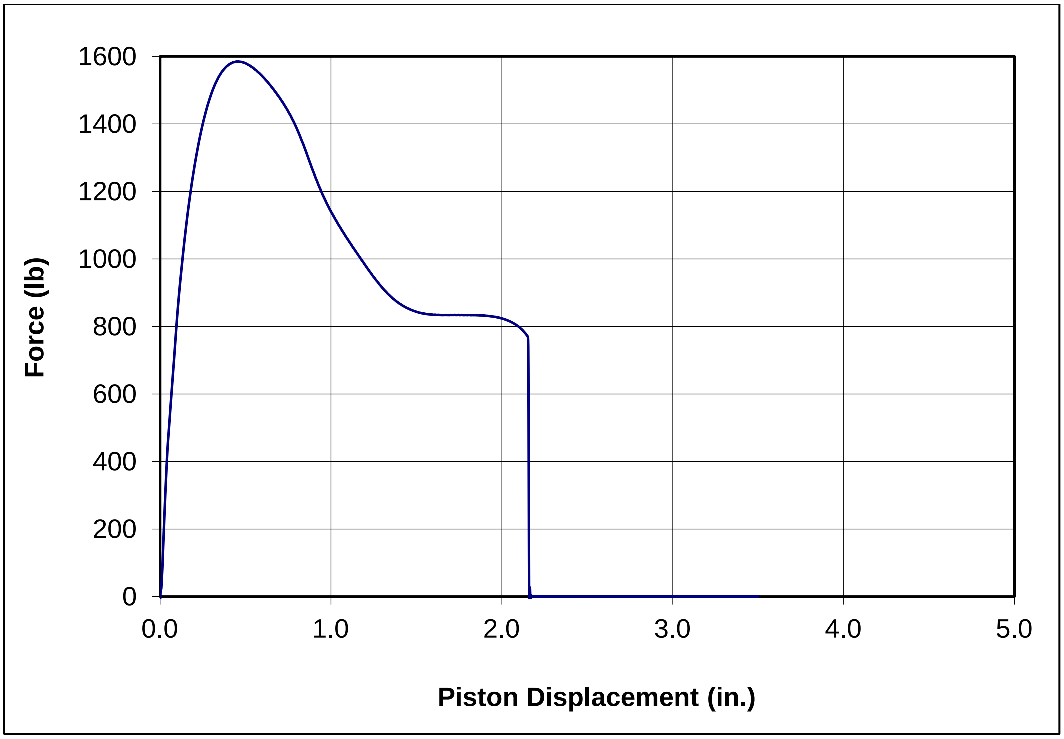

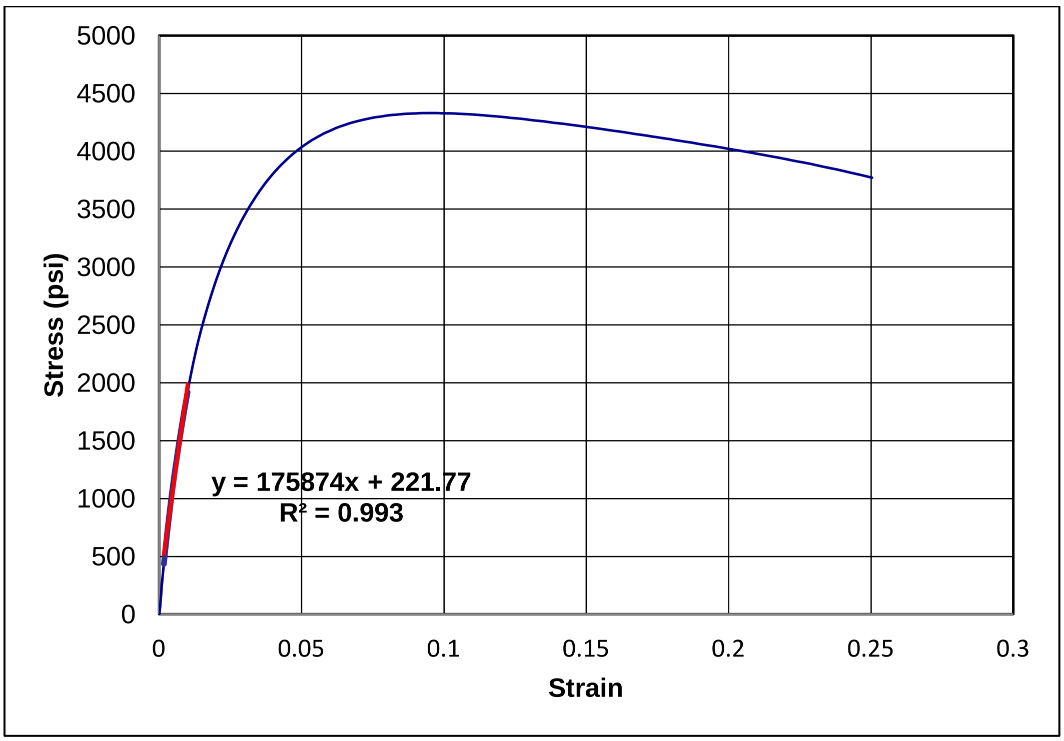

Figure 6. Typical force-displacement plot (*upper*) and stress-strain plot (*lower*) for Vendor B HMW-PE specimens (specimen B-21: 23°C and 20 in./min). Tensile stress at yield was the maximum stress for all test specimens.

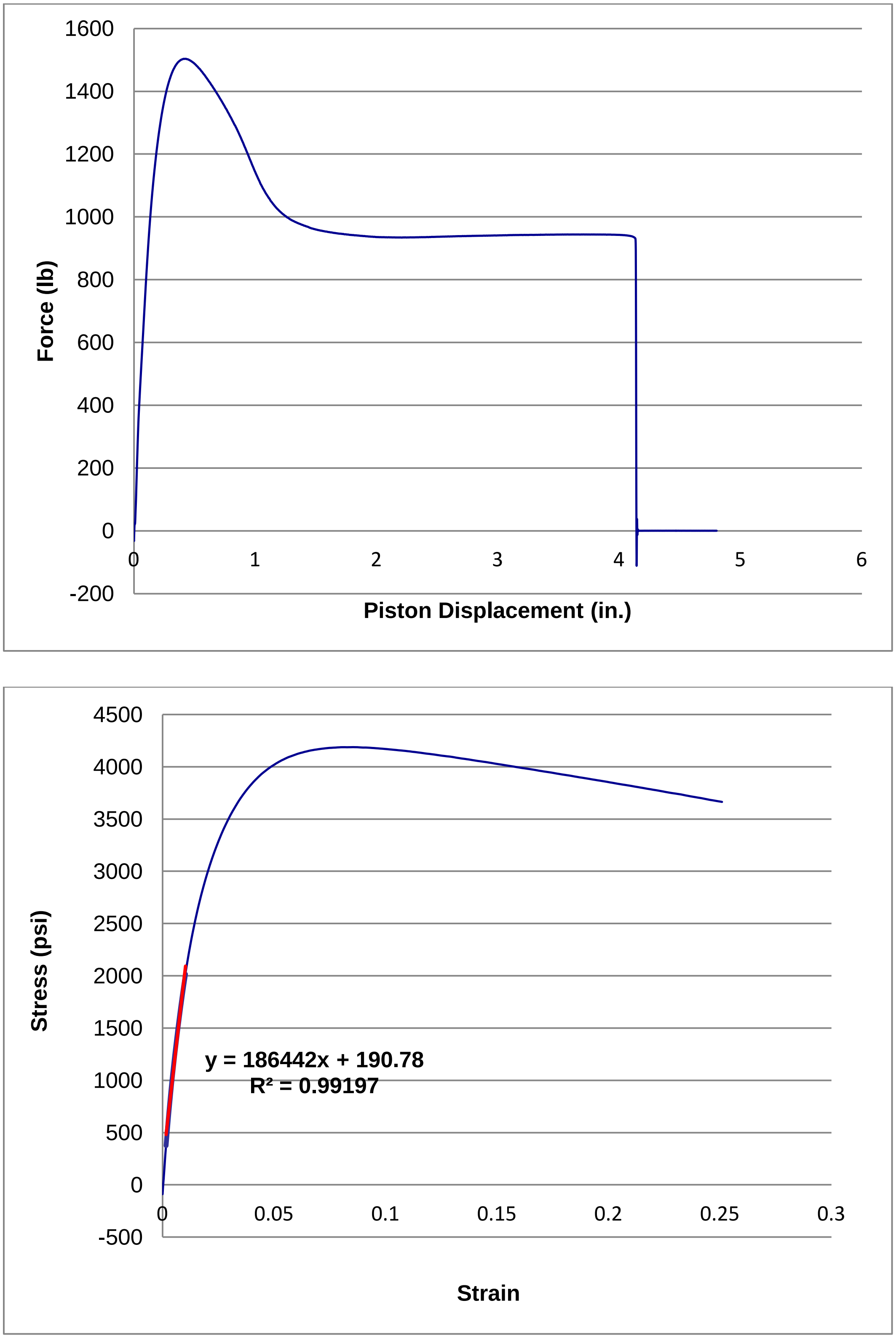

Note that elongation within the gage length always exceeded the range of the clip-on extensometer (0.5 in.), whereupon a pin released to prevent damage to the device. Consequently, we used crosshead or piston displacement, via LVDT data, to determine EAB for all specimens, with percent elongation obtained by dividing by the length of the narrow section, L = 2.25 in. ASTM (2010) D638 acknowledges that separate methods are likely needed to measure the small displacements for Young's modulus and large displacements at break for many plastics. By dividing by 2.25 in. to obtain percent EAB, we treat all elongation as if it occurred within the narrow section of the specimen. This is certainly not true up to the yield point as elastic strain also occurs outside of the narrow section. Nevertheless, EAB is several times larger than at yield; and the wide ends of the specimen probably relax elastically after the narrow section begins to weaken. That is, crosshead displacement is probably a good approximation of elongation within the narrow section at the moment that the specimen breaks.

As with any test program, we encountered a few challenges while conducting the tests, and Appendix D identifies them for each test. The most significant issue was that some of the new, unused samples slipped out of the grips before reaching maximum stress. The slipping was due to insufficient clamping pressure of the manual vise grips and occurred 10 times with the Vendor A specimens and 8 times with the Vendor B specimens. None of these specimens appeared to have yielded or necked prior to slipping and were subsequently placed back in the grips and re-tested until no slipping occurred. Extensometer data later confirmed that essentially all elongation was recovered when the specimens slipped. Because only elastic deformation apparently occurred, we included results of subsequent successful tests in calculating series average tensile stresses and elongations. We used the extensometer data from the initial pull for modulus calculations in all cases, whether or not slipping occurred.

As seen in Table 4, standard deviations for all Vendor A test series were small relative to average values for all properties measured. This probably reflects homogeneity of the HMW-PE samples and consistency of specimen preparation and test methods. An exception was one of six field-series specimens, AFS-6. While its Young's modulus and yield stress were consistent with series averages, the specimen broke abruptly at its yield point. Consequently, we excluded its values from series averages but discuss this behavior in more detail in Section 6.

There were two important exceptions affecting the Vendor B results in Table 5. One of the five specimens tested at room temperature, B-23, did not break at the full 6 in. elongation possible in the tests. We therefore only included its yield stress in series averages.

The other Vendor B exception was one of six field-series specimens, BFS-5. While its Young's modulus and yield stress were consistent with series averages, the specimen broke at a much lower stress (890 psi) and somewhat lower elongation (26%) than series averages (2900 psi and 36%, respectively). We included these values in series averages and discuss their implications in more detail in Section 6.

Figures 7 and 8 show the effects of temperature on average yield stress and on Young's modulus for new, unused samples at a constant crosshead rate of 20 in./min. Both values increase nearly linearly with decreasing temperature over the test range of 23 to −40°C. The field specimens tested at −40°C and 20 in./min plot on top of the new, unused results. The HMW-PE material clearly stiffens and becomes stronger at lower temperatures.

Figure 7. Average yield (maximum) stress versus temperature for Vendor A and B specimens tested at a 20 in./min crosshead speed. Error bars show ± one standard deviation.

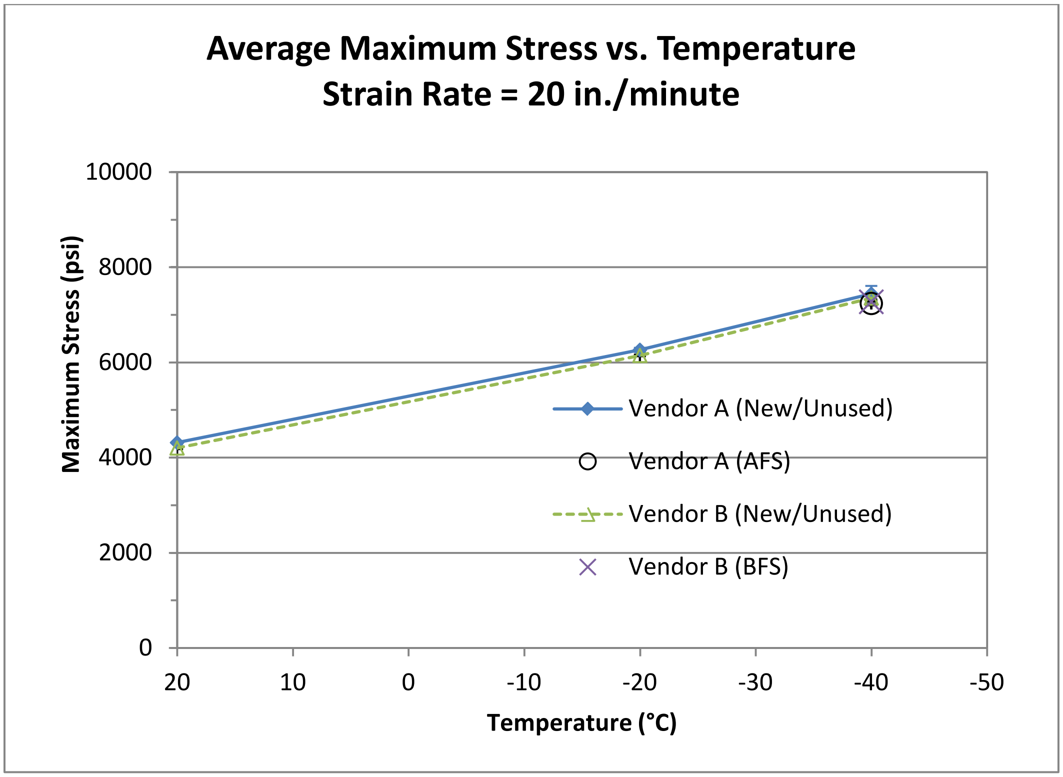

Figure 8. Average Young's modulus versus temperature for Vendor A and B specimens tested at a 20 in./min crosshead rate. Error bars show ± one standard deviation.

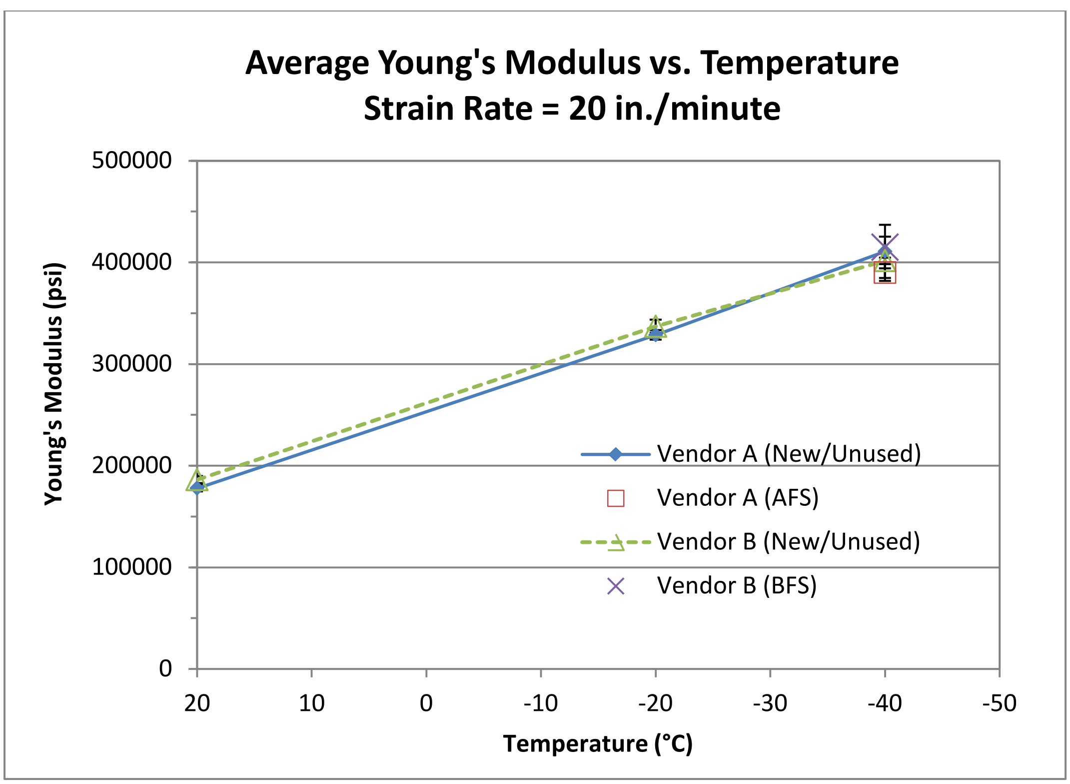

Figures 9 and 10 show the average yield stress and Young's modulus versus crosshead rate at a constant −40°C. Over the test range 20 to 80 in./min, both values are essentially independent of rate for new, unused specimens.

Figure 9. Average yield (maximum) stress versus crosshead rate for Vendor A and B specimens tested at −40°C.

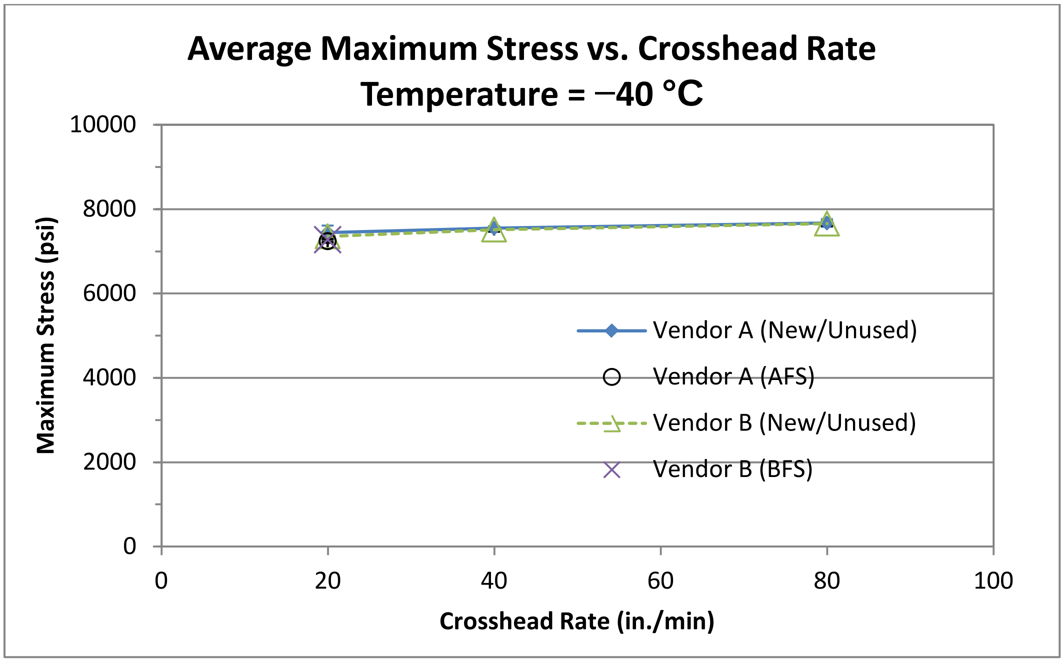

Figure 10. Average Young's modulus versus crosshead rate for Vendor A and B specimens tested at −40°C.

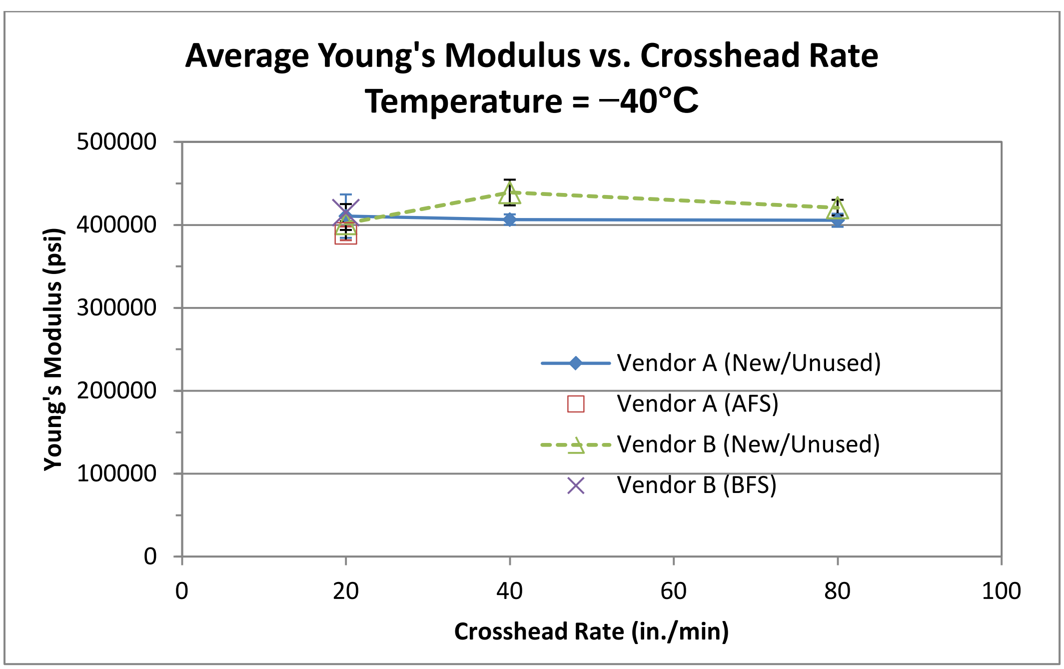

Figures 11 and 12 show the effects of temperature and crosshead rate, respectively, on failure stress. While crosshead rate again has little influence, failure stress increases with decreasing temperature over the test range 23°C to −40°C. Average failure stress for field specimens was slightly lower than new, unused specimens at −40°C and 20 in./min, and more variability occurred.

Figure 11. Average failure stress versus temperature for Vendor A and B specimens tested at 20 in./min crosshead rate.

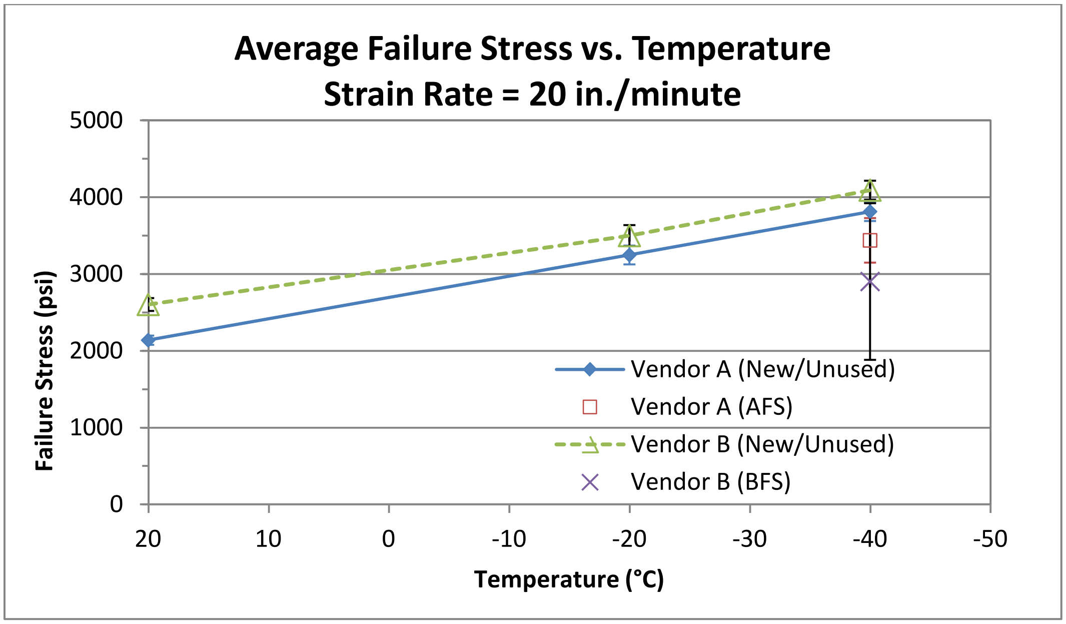

Figure 12. Average failure stress versus crosshead rate for Vendor A and B specimens tested at −40°C.

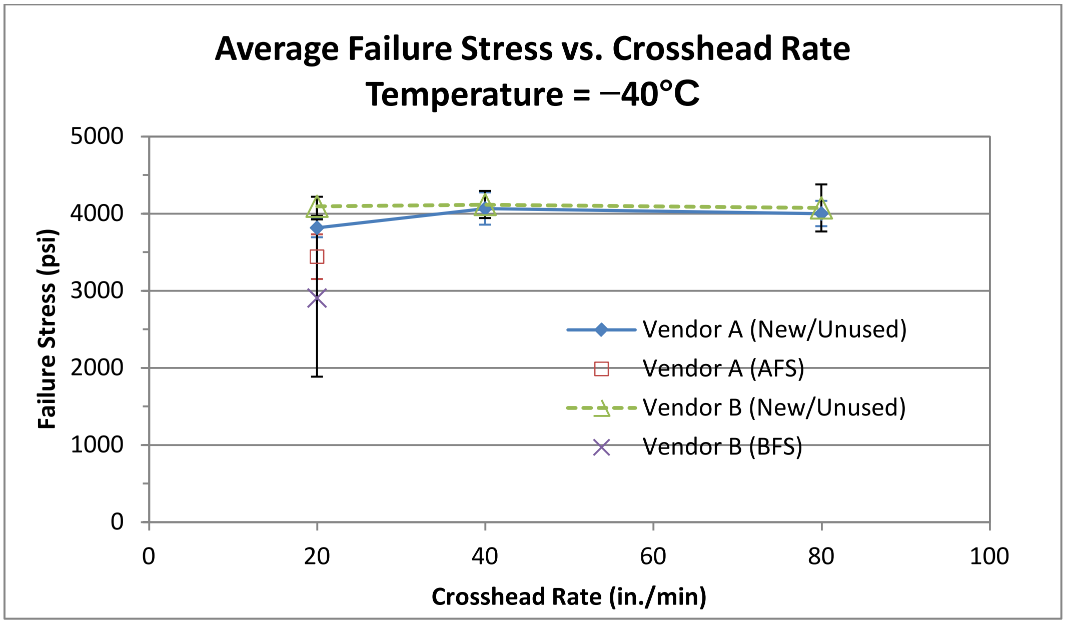

Figures 13 and 14 show the effects of temperature and crosshead rate, respectively, on percent EAB. Again, crosshead rate had little effect, but EAB decreases dramatically with decreasing temperature over the test range 23°C to −40°C. It is interesting to note in Figure 14 that the Vendor B field specimens showed much lower EAB compared with new, unused specimens at −40°C and 20 in./min.

Figure 13. Average elongation at break versus temperature at 20 in./min crosshead rate for Vendor A and B test series.

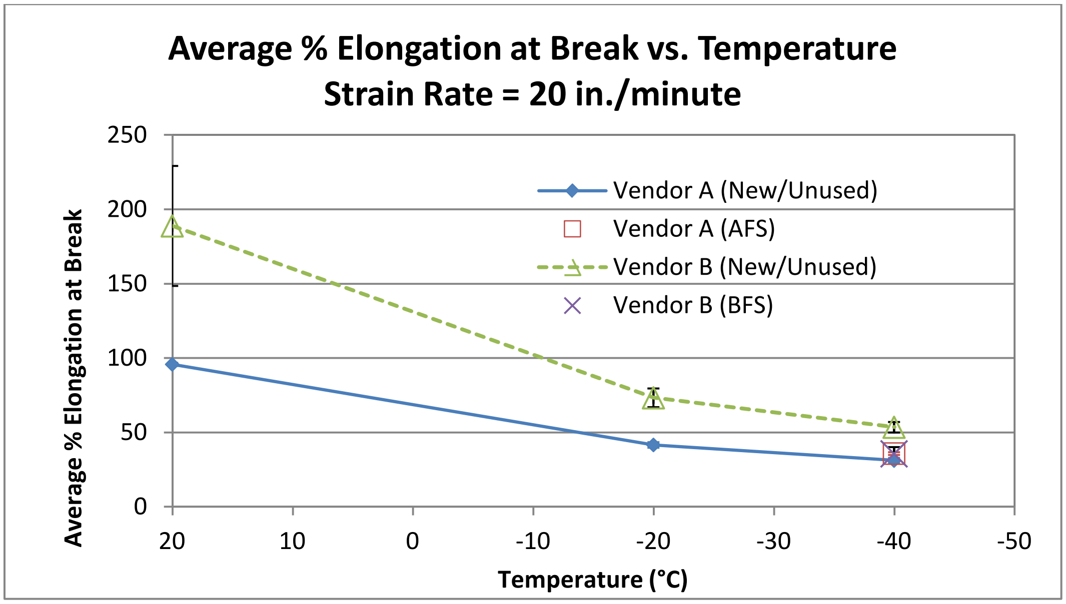

Figure 14. Average elongation at break versus crosshead rate for Vendor A and B specimens tested at −40°C.

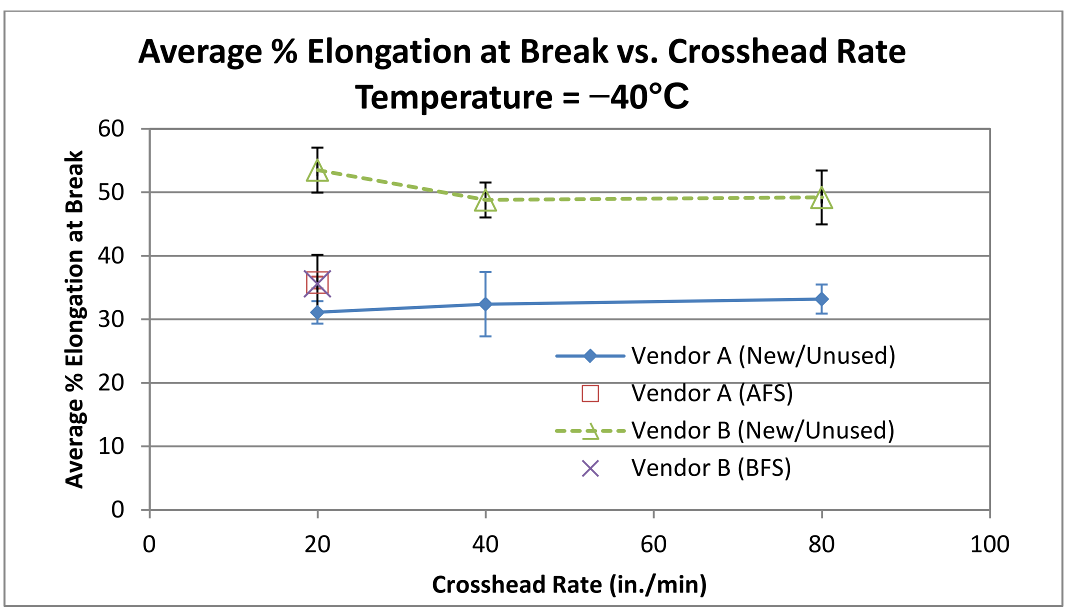

Both new, unused specimens and field specimens from Vendor A showed very little necking prior to failure (Figure 15). In addition, the specimens exhibited discoloration, or "crazing," and splits or discontinuities at the failure surface (Figure 16). In both respects, the field specimens behaved similarly to the new, unused specimens.

Figure 15. Necking behavior of new, unused specimens (*upper*) and field specimens (*lower*) for Vendor A HMW-PE tests conducted at −40°C and 20 in./min. Little necking occurred for all tests except those conducted at room temperature.

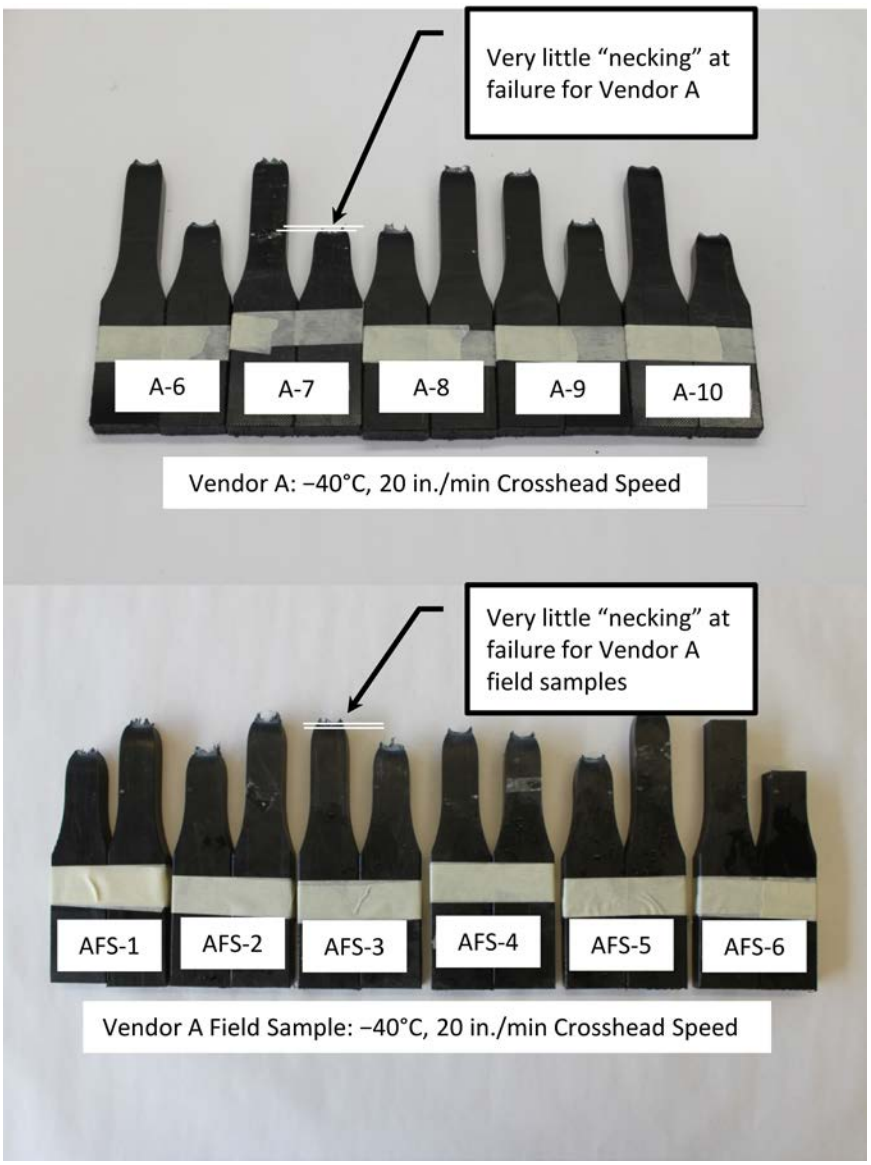

Figure 16. Splitting and crazing of Vendor A HMW-PE at failure surfaces of a new, unused specimen (*upper*) and a field specimen (*lower*) tested at −40°C and 20 in./min.

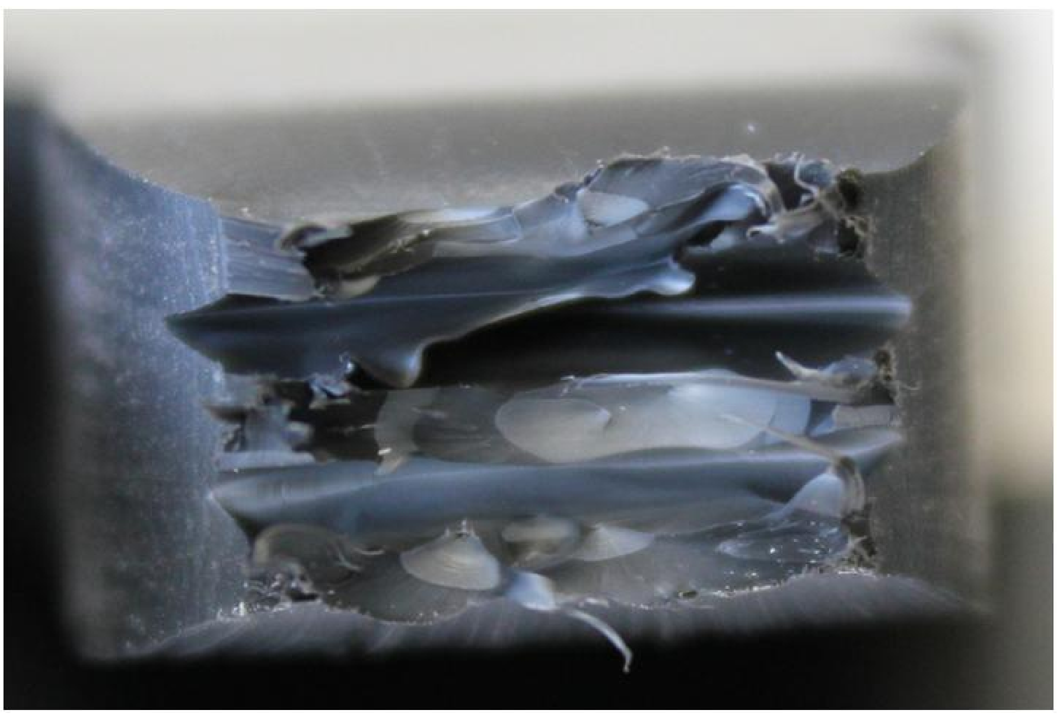

The new, unused Vendor B specimens displayed significant necking (Figure 17, *top*) and fairly uniform failure surfaces with little crazing and few splits or discontinuities at the failure surface (Figure 18, *top*). By comparison, the Vendor B field specimens showed little necking prior to failure (Figure 17, *bottom*) and significant crazing and splitting at the failure surface (Figure 18, *bottom*).

Figure 17. Necking behavior of new, unused Vendor B HMW-PE specimens (*upper*) and field specimens (*lower*) for tests conducted at −40°C and 20 in./min. The new, unused specimens displayed more necking and more uniform failure surfaces compared with the field specimens.

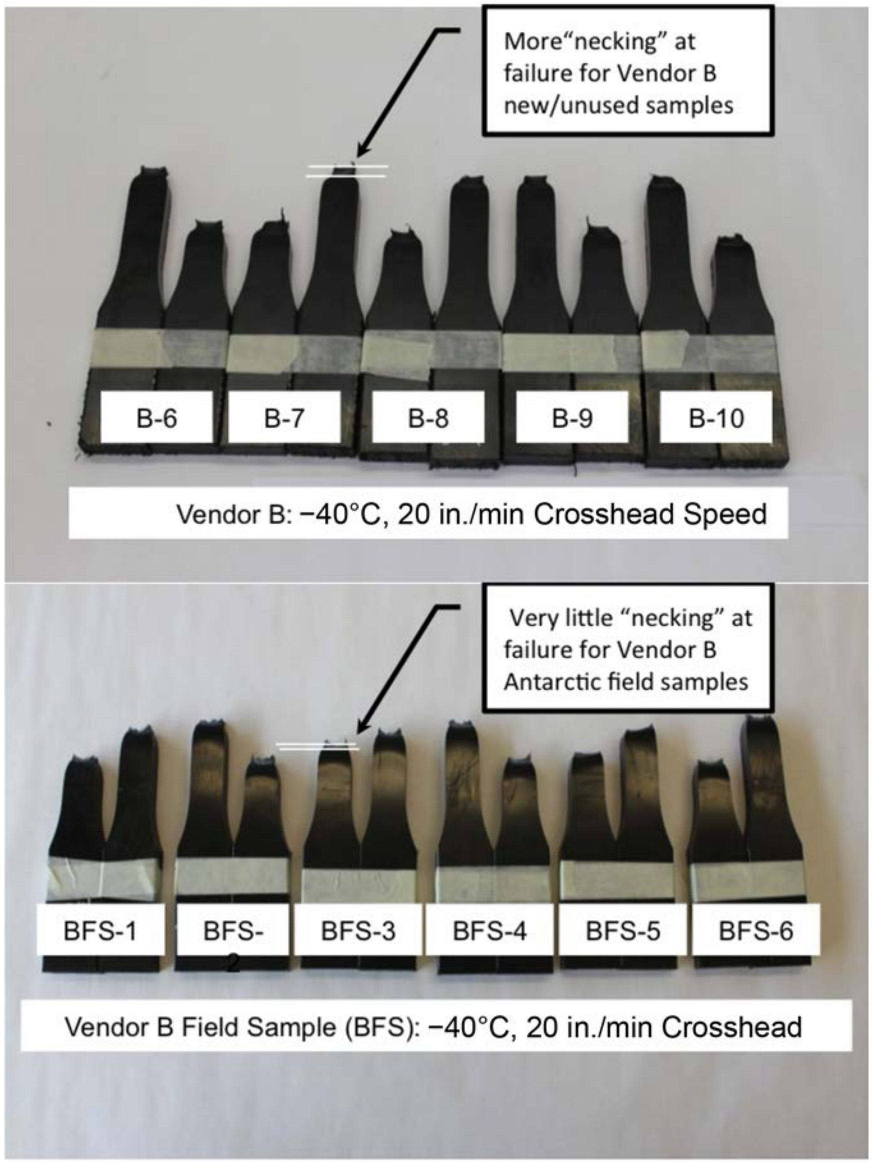

Figure 18. Well-defined necking and a fairly uniform failure surface of new, unused Vendor B HMW-PE specimen (*upper*) compared with little necking and significant splitting and crazing at the failure surface of a Vendor B HMW-PE field specimen (*lower*), both tested at −40°C and 20 in./min.

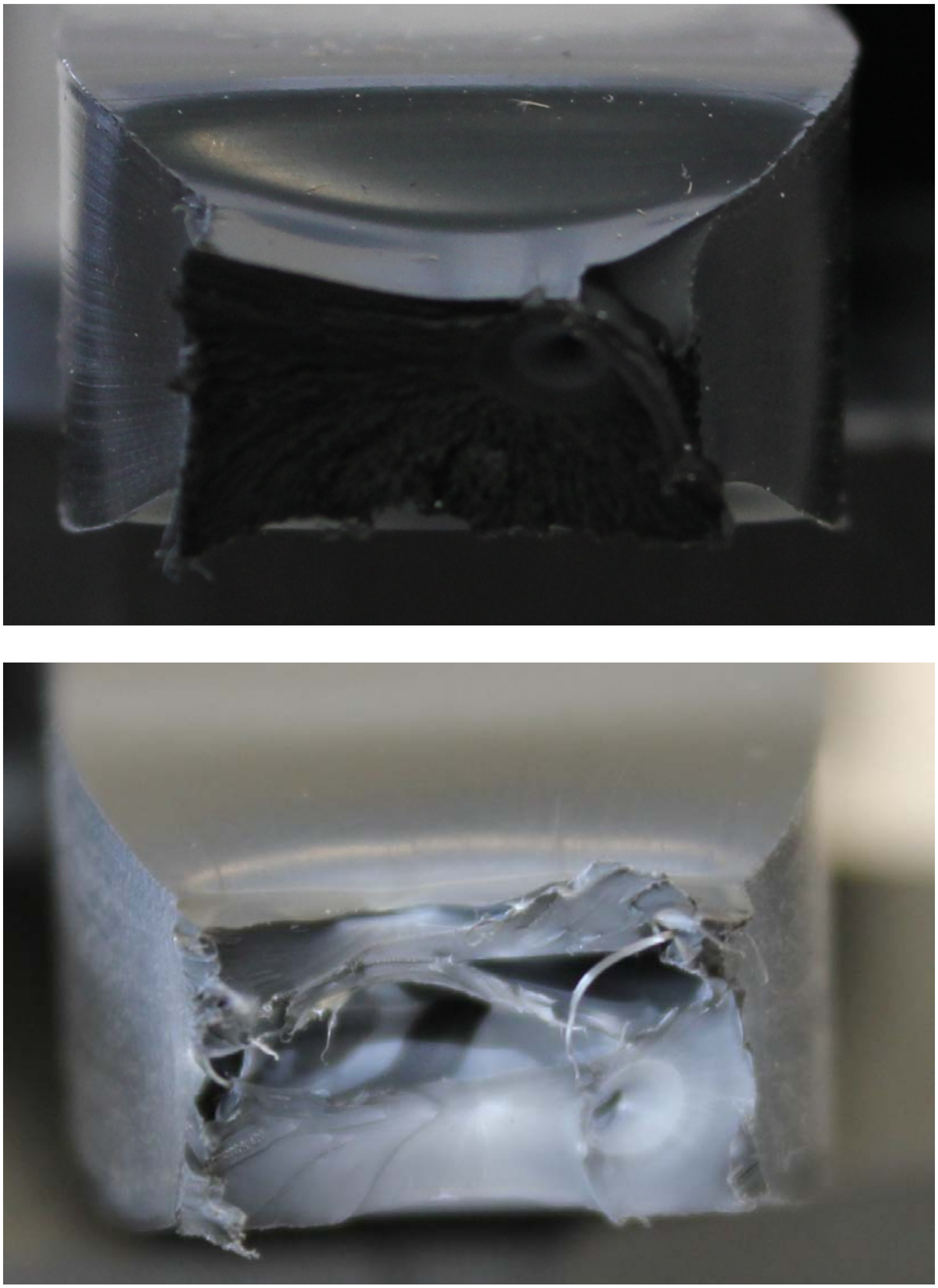

6 Findings and Recommendations from the Test Program

We conducted tensile tests of 0.5 in. thick, black HMW-PE samples from two vendors to help understand the behavior of large sheets as part of flexible fuel-bladder sleds used in Antarctic and Greenland. We obtained new, unused Vendor A samples from the same production run as HMW-PE sheets supplied to SPoT in 2010 and also obtained a sample of a sheet that failed during its first year of service on SPoT.

We also obtained new, unused Vendor B samples from the same production run as HMW-PE sheets supplied to SPoT in 2009, and we obtained a sample of a sheet that survived the subsequent two years of service on SPoT.

Insofar as possible, we followed ASTM D638, *Standard Test Method for Tensile Properties of Plastics* (ASTM 2010), to prepare the specimens and to conduct the tests. Except for a baseline series at room temperature, test conditions reflected a range of service conditions (−20°C to −40°C, 20 to 80 in./min) appropriate for polar traverses. The consistency of the test results, as reflected in similar force-displacement records and low standard deviations on average outcome values, suggest good execution of the tests.

Over the range of conditions tested, temperature influenced HMW-PE behavior for both the Vendor A and Vendor B specimens much more than crosshead rate did. Comparing average tensile properties for Vendor A and Vendor B samples, respectively, at room temperature and at −40°C (at a common 20 in./min crosshead rate), yield stress increased 72% and 75%, failure stress increased 79% and 57%, and Young's modulus increased 130% and 116%. That is, both materials became much stiffer and stronger at low temperature. However, they also became much less ductile: EAB dropped by more than a factor of 3, from 96% to 31% and 189% to 54%, respectively, for Vendor A and Vendor B samples.

Tensile properties listed in the vendor specification sheets (Appendix A) also conform to ASTM (2010) D638. Although not noted, tests would likely have been conducted at room temperature and could have been at a crosshead rate as slow as 0.2 in./min. The listed yield stress for Vendor A HMW-PE (3600 psi) is similar to that obtained here at room temperature (4320 psi). However, the listed EAB is much larger, more than 600% compared with 96% here. This represents a substantial reduction in ductility of the material, even at room temperature, presumably owing to our use of a higher crosshead rate. With even less ductility at −40°C, it is not surprising that failures in Vendor A HMW-PE sheets used in Antarctica were more similar to brittle failures rather than ductile ones.

The data reported on the Vendor B specification sheet were for ASTM (2010) D638 tensile tests conducted at a 2 in./min crosshead rate and were likely at room temperature. The listed yield stress for Vendor B plastic (3625 psi) is similar to that obtained here at room temperature (4200 psi). However, the listed EAB is much larger, a minimum of 600% compared with 189% measured here. We should note that one room temperature Vendor B specimen did not fail at full elongation (approximately 300%); our reported average would have been higher with its inclusion. Nevertheless, this represents a substantial reduction in ductility of the material, even at room temperature, presumably owing to our use of a higher crosshead rate. Our investigations appear to predict that with even less ductility at −40°C, Vendor B HMW-PE sheets used in Antarctica and Greenland could experience brittle failures similar to Vendor A.

An important consequence of reduced ductility is that the HMW-PE sheets become much more sensitive to manufacturing defects, introduced via the extrusion and cooling processes, and to scratches resulting from field handling (especially unrolling) at low temperatures. The overall strength of brittle materials is strongly influenced by the distribution of flaws that can nucleate cracks. For HMW-PE sheets measuring 8 ft wide × 68 ft long, flaws combined with brittle behavior could prove catastrophic to traverse operations. Locally high, short-term stresses would fail a brittle sheet much more easily than a ductile one.

We found some evidence for this concern within the specimens prepared from a Vendor A HMW-PE sheet that failed during its first season on SPoT and also within the specimens prepared from a Vendor B HMW-PE sheet that completed two full seasons on SPoT. One of the six Vendor A specimens tested at −40°C and 20 in./min (AFS-6) failed abruptly at its yield point. Because this specimen had similar yield stress and Young's modulus as the series averages, the test was probably a valid one. This specimen also had no visual external flaws. Its brittle failure could reflect the fatal combination of internal flaws and reduced low-temperature ductility potentially responsible for HMW-PE sheet failures in Antarctic sleds.

Both tensile strength and EAB of the Vendor B field samples averaged about 70% lower than new, unused specimens tested at the same conditions (−40°C and 20 in./min). This could be a consequence of UV exposure or other, undetermined, service conditions. Furthermore, one of the six specimens tested at −40°C and 20 in./min (BFS-5) displayed less elongation and much lower stress at break than series averages. Because this specimen had similar yield stress and Young's modulus as the series averages, the test was also probably a valid one. As with the Vendor A plastic, this Vendor B specimen had no visual external flaws, and its post-yield performance could also reflect the fatal combination of internal flaws and reduced low-temperature ductility potentially responsible for HMW-PE sheet failures in polar sleds.

The specified "brittleness temperatures" for Vendor A and Vendor B HMW-PE are less than −90°C and less than −118°C, respectively, based on ASTM D746 (Appendix A). Nevertheless, the materials displayed significantly reduced ductility at −40°C, as measured using tensile test method ASTM (2010) D638. Furthermore, a higher Young's modulus measured at low temperatures would imply higher stresses as sheets attempt to conform to sharp-crested sastrugi. Clearly, dedicated tensile tests of the type conducted here were necessary to capture changes in HMW-PE mechanical properties relevant to Antarctic and Greenland flexible sleds.

We postulate that EAB, as measured using ASTM (2010) D638 uniaxial tensile tests at −40°C and 20 in./min, is a suitable index to characterize ductility and hence the likely in-service performance of HMW-PE sheets used for polar bladder sleds. As evidence, we note high initial failure rates of 13% and 50% during the first year of field service for Vendor A and Vendor C HMW-PE sheets, respectively. These brand-new materials had relatively low EAB averages of 31.1% and 39.1%, respectively. Conversely, Vendor B HMW-PE new material averaged a much higher 53.5% EAB, and all four of these sheets survived two years of field service.

Based on this initial test series, completed in 2011, we recommended that SPoT and GrIT establish material specifications for HMW-PE sheet procurements, including a minimum of 50% EAB, as measured using ASTM (2010) D638 uniaxial tensile tests at −40°C and 20 in./min.

In addition, we recommended that samples be taken from in-service HMW-PE sheets, pre- and post-season, to track possible reductions in ductility through ASTM (2010) D638 uniaxial tensile tests. We noted that average EAB of Vendor B HMW-PE specimens dropped to 35.6% after two years of service, a value bracketed by those for failure-prone Vendor A and Vendor C sheets.

In addition, we recommended that CRREL, on behalf of SPoT and GrIT, interact with interested HMW-PE manufacturers to determine whether they would be willing to revise their HMW-PE formulations to improve the ductility of sheets procured for bladder sleds.

NSF-PLR, SPoT, and GrIT adopted these recommendations.

7 A Plan to Reduce In-Service Sled Failures

Large HMW-PE sheets used for polar flexible sleds need significant low-temperature ductility to reduce their sensitivity to internal flaws and damage caused by rough handling or heavy equipment. Initial discussions with vendors indicated that it might be possible to alter the material mix or manufacturing method to achieve greater ductility at low temperature, perhaps by trading off high-temperature performance not required for this application. However, even though the vendors suggested that they could work to improve performance, mix proportioning and design are proprietary information. Hence, the sled development process would have to be guided by establishing performance specifications and testing the products against those specifications. We proposed using EAB, as measured using ASTM (2010) D638 uniaxial tensile tests at −40°C and 20 in./min, as the measure of ductility.

We expected that this would be a lengthy process: establish a near-term goal within reach of existing materials, encourage interested vendors to modify their HMW-PE formulations to exceed that goal, test the revised mixes in the lab using ASTM (2010) D638 as before, place the best performing material in service in Antarctica and Greenland, track in-field failure rates, and test samples of the in-service sleds after each season to document any changes in ductility. Adding to the challenge was the fact that each vendor required a minimum order prior to committing to the design and production of a modified product. This seemed a reasonable compromise: the vendors would bring their expertise to bear on our need for low-temperature ductility, and SPoT and GrIT would combine to purchase the necessary minimum quantities.

Both Vendor A and Vendor B chose to participate in this development effort. Vendor C opted out. Vendor C had provided sled material to GrIT in 2010, and it had quickly failed in the field. Of course, there are tradeoffs when altering polymer formulation, and enhanced ductility could potentially reduce other performance factors, such as strength and elastic modulus. The lab tests would continue to measure these parameters.

Our initial study revealed that EAB above 50% was achievable for an existing HMW-PE formulation and would provide longer service life than material with an initial EAB of 30%–35%. We could, therefore, set 50% as the minimum specification and rate new formulations against that target but be assured that at least one vendor could supply sleds that met the minimum.

We implemented this approach with the support of NSF-PLR and the prime contractors responsible for executing SPoT and GrIT. We established a common set of specifications for HMW-PE sleds, and the contractors agreed to combine procurements to exceed minimum orders of revised material from each vendor. The procurement contracts required that samples be cut from the production runs and sent directly to our laboratory for testing. The first revisions from each vendor were delivered to CRREL and tested in 2011, and each vendor subsequently made a second set of plastic-mix revisions and delivered those samples in 2012. The following sections of this report present test results of the revised HMW-PE formulations, assess sled degradation due to field service, correlate EAB values with in-service failure rates, establish revised specifications for material acceptance, and suggest a guideline for planned removal from service to avoid in-field sled failures.

8 Revised HMW-PE Formulations

Both vendors sent production samples of their revised HMW-PE formulations for testing at CRREL. Our aims were to compare tensile-test results against values from "original" COTS mixes. This would help us to establish baseline material properties against which to compare returned samples from the field to monitor degradation with environmental exposure and use. The new plastic samples were prepared for tensile tests following the methods described in Section 4. We tested all specimens at −40°C and a 20 in./min crosshead rate.

The revised HMW-PE formulations performed better in terms of the principal metric, EAB, than the COTS products from both vendors. Table 6 summarizes the test results. The 2011 Revision 1 for Vendor A (AR1) improved to an initial (new, unused) EAB of 61.8% from 31.1% in its original form. Vendor B's 2011 material (BR1) measured 58.6% versus 53.5% in its original mix. Both revised mixes showed slightly lower tensile strengths (8%–10%), but both materials maintained safety factors exceeding 30 relative to peak towing stresses (about 200 psi). A small reduction in tensile strength seemed a reasonable tradeoff to obtain increased low-temperature ductility. Based on our recommendations, SPoT procured and placed into service 34 sheets of BR1 for its 2011–12 season. For 2012, GrIT and SPoT each procured four sheets of AR1 and placed them into service.

In 2012, both vendors thought they could make further ductility gains in their HMW-PE formulations without compromising other physical properties. We designated these formulations AR2 and BR2 and tested samples from each (Table 6). New, unused AR2 achieved EAB of 63.0%; and new, unused BR2 achieved a value of 77.4%. These represent very substantial improvements in low-temperature ductility compared with their original products (31.1% and 53.5%, respectively). For its 2012–13 season, SPoT procured and placed into service 12 sheets of BR2 and six sheets of AR2.

Table 6. Laboratory results of ASTM (2010) D638 tensile tests of production run, unused HMW-PE samples from three vendors. Note that all tests were conducted at −40°C and 20 in./min load rate.

Source Material	Production Year	Age	Elongation at Break (%)	Standard Deviation (%)	Tensile Stress at Yield (psi)
Vendor A: original	2010	New	31.1	1.8	7440
Vendor A: AR1	2011	New	61.8	3.9	6669
Vendor A: AR2	2012	New	63.0	3.9	6434
Vendor B: original	2009	New	53.5	3.5	7360
Vendor B: BR1	2011	New	58.6	3.2	6789
Vendor B: BR2	2012	New	77.4	9.9	7010
Vendor C: original	2010	New	39.1	1.4	7063

The tensile-test results for revised HMW-PE formulations were encouraging. Both vendors achieved greater low-temperature ductility within the constraints of their mix formulations and production processes and without significant losses in tensile strengths. The revised products also looked as smooth and glossy as the original HMW-PE materials, suggesting that they would perform efficiently as sleds. What remained was to determine whether or not the gain in initial ductility could stand-up to field service and thereby extend sled service life.

One possible concern was the standard deviation of Vendor B's 2012 BR2 mix. At 9.9%, it was approximately three times higher than all of the other measured standard deviations. High variances within a single production run, or between productions of the same mix, could lead to random field-service failures and thus yield unpredictable HMW-PE service life.

9 Assessing HMW-PE In-Service Performance

In 2011, we embarked on a program to monitor the in-service performance of all HMW-PE sled formulations. We intended to conduct tensile tests, following ASTM (2010) D638 and testing at −40°C and 20 in./min crosshead rate, of sled samples returned from the field. This would allow some insight into changes in ductility with field exposure. We also continued to track in-service failure rates to assess whether specimen-average EAB provided a useful index of sled durability. Our hope was that we might identify a minimum allowable EAB value below which sleds from that production run must be retired from service to avoid costly and time-consuming in-service sled failures.

SPoT developed a sled-identification system so that individual sleds of each production run could be tracked. Field crews then cut samples from the exposed rear corners of representative sleds. The samples were returned to CRREL for tensile testing.

We established a time scale to compare HMW-PE performance as a function of in-service age. For this purpose, we consider a trip from McMurdo to South Pole equivalent to 0.25 service years. Similarly, a return trip from South Pole to McMurdo is 0.25 service years. This allows for cases where HMW-PE sheets are placed in service at either location. An austral winter is considered equivalent to 0.5o service years. Often, we obtained samples cut from sheets at South Pole Station after an outbound trip and again upon return from to McMurdo (0.5 years total). The field crew has also cut samples in the austral spring (October) following over-winter outdoor storage (1.0 years total).

Table 7 compiles the SPoT and GrIT in-service sled failure rates for all HMW-PE production runs, including original white sheets. An in-service failure is defined as an abrupt fracture of the HMW-PE sheet under normal use, and it renders the sheet unusable. It is usually not known whether the failure occurred at a previously damaged location (e.g., a scratch acquired during sheet unrolling), but the crew makes every effort to minimize handling damage. Table 8 summarizes the tensile-test results by production run and service age. It also includes in-service failure rates for the season immediately subsequent to the tests.

Table 7. The number of in-service HMW-PE sheets (68 ft length) and corresponding in-service failure rates compiled by SPoT and GrIT season and HMW-PE production run.

Season	Source Material	In-Service Sheets	Failure Rate
White HMW-PE			
GrIT08	Vendor A: white	3	0%
SPoT08-09	Vendor A: white	35	26%
SPoT09-10	Vendor A: white	24	71%
GrIT10	Vendor A: white	3.5	0%
Black HMW-PE			
SPoT09-10	Vendor B: original	4	0%
SPoT10-11	Vendor B: original	4	0%
SPoT10-11	Vendor A: original	24	13%
GrIT11	Vendor B: original	6	0%
GrIT11	Vendor C: original	2	50%
SPoT11-12	Vendor B: original	4	50%
SPoT11-12	Vendor A: original	5	60%
SPoT11-12	Vendor B: BR1	34	0%
SPoT11-12	Vendor A: original	6	0%
GrIT12	Vendor B: original	6	0%
GrIT12	Vendor A: AR1	4	0%
SPoT12-13	Vendor B: BR1	34	0%
SPoT12-13	Vendor A: AR1	4	0%
SPoT12-13	Vendor B: BR2	12	0%
SPoT12-13	Vendor A: AR2	6	0%
SPoT13-14	Vendor B: BR1	34	0%
SPoT13-14	Vendor A: AR1	4	0%
SPoT13-14	Vendor B: BR2	12	0%
SPoT13-14	Vendor A: AR2	6	0%
GrIT14	Vendor B: original	6	0%
GrIT14	Vendor A: AR1	4	0%

Table 8. Laboratory results of ASTM (2010) D638 tensile tests of HMW-PE samples from three vendors while in field service. Note that all tests were conducted at −40°C and 20 in./min load rate.

Source Material	Production Year	Service Age at Test	Elongation at Break (%)	Standard Deviation (%)	Tensile Stress at Yield (psi)	In-Service Failure Rate (%)
Vendor A: original	2010	New	31.1	1.8	7440	13%
		0.5	35.8	0.9	7240	60%
Vendor A: AR1	2011	New	61.8	3.9	6669	0%
		1	58.1	7.9	6478	0%
		1.5	58.3	2.7	6194	0%
		2	39.7	1.3	7026	0%
Vendor A: AR2	2012	New	63.0	3.9	6434	0%
		1	60.8	3.5	6245	0%
Vendor B: original	2009	New	53.5	3.5	7360	0%
		1	Not measured	Not measured	Not measured	0%
		2	35.6	4.6	7280	50%
		2.5	36.7	1.7	7270	0%
Vendor B: BR1	2011	New	58.6	3.2	6789	0%
		1	65.8	9.1	7047	0%
		1.5	65.5	4.5	7073	0%
		1.75	49.8	2.9	7285	0%
		2	60.9	2.0	7091	0%
Vendor B: BR2	2012	New	77.4	9.9	7010	0%
		1	56.7	3.4	6792	0%
Vendor C: original	2010	New	39.1	1.4	7063	50%

Figure 19 plots the measured EAB versus in-service failure rates for all production runs of HMW-PE for SPoT and GrIT. No in-service failures have occurred for sheets with measured EAB above 40%. Below this value, high in-service failure rates have occurred, including for sheets newly placed into service. The data suggest that 40% EAB, as measured using ASTM (2010) D638 tensile tests conducted at −40°C and 20 in./min, represents a threshold below which HMW-PE sheets should be removed from service.

Figure 19. In-service sled failure rates versus elongation at break for specimens obtained prior to the field season. The results are for all production runs of HMW-PE tested and for SPoT and GrIT in-service failures.

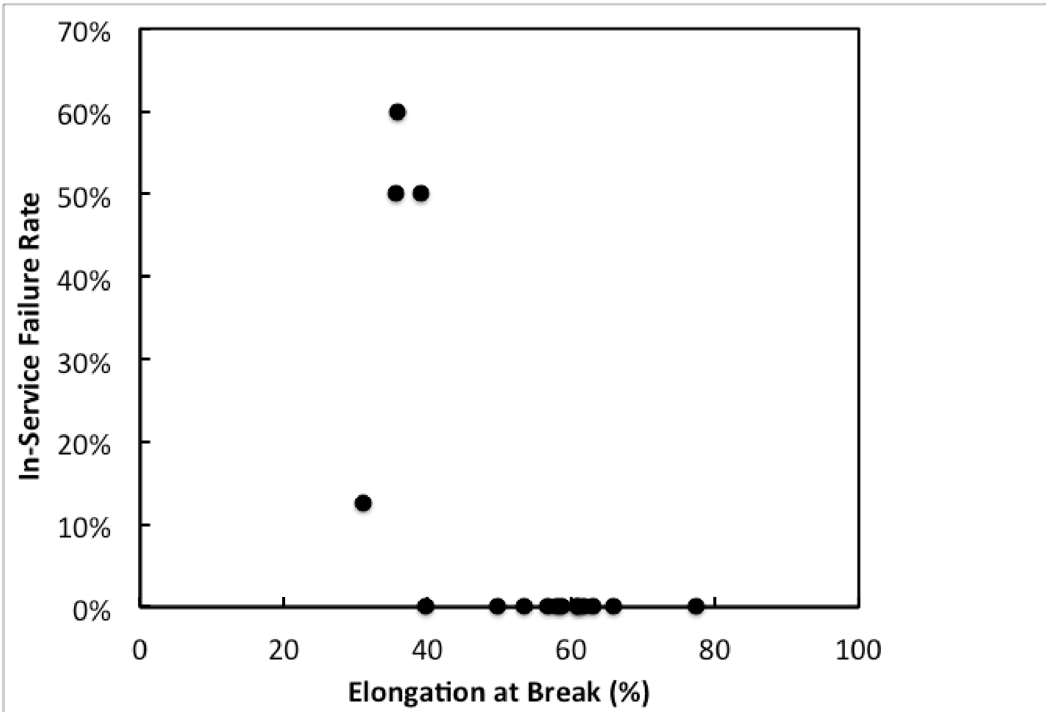

Figure 20 plots variations in EAB versus sled in-service age. Although much scatter exists, it is possible that EAB decreases with service age because of environmental or operational effects (e.g., UV exposure, repetitive flexing over sharp sastrugi, scratches from mobilization and demobilization equipment, etc.). The plot includes the 40% threshold value where in-service failure rates increase. The most recent formulations (AR2 and BR2) both show greater than 60% EAB when new, which allows for some loss in ductility with service age before reaching the 40% threshold. By tracking changes in EAB with service age, we hope to compare the relative performance of the various HMW-PE formulations and estimate likely service life for each production run of HMW-PE sheets.

Figure 20. Measured elongation at break versus sled service age for each HMW-PE production run. The lower dashed line is the 40% value considered as a threshold to avoid high failure rates. The upper dashed line at 60% is an achievable initial specification for Vendors A and B's revised HMW-PE formulations.

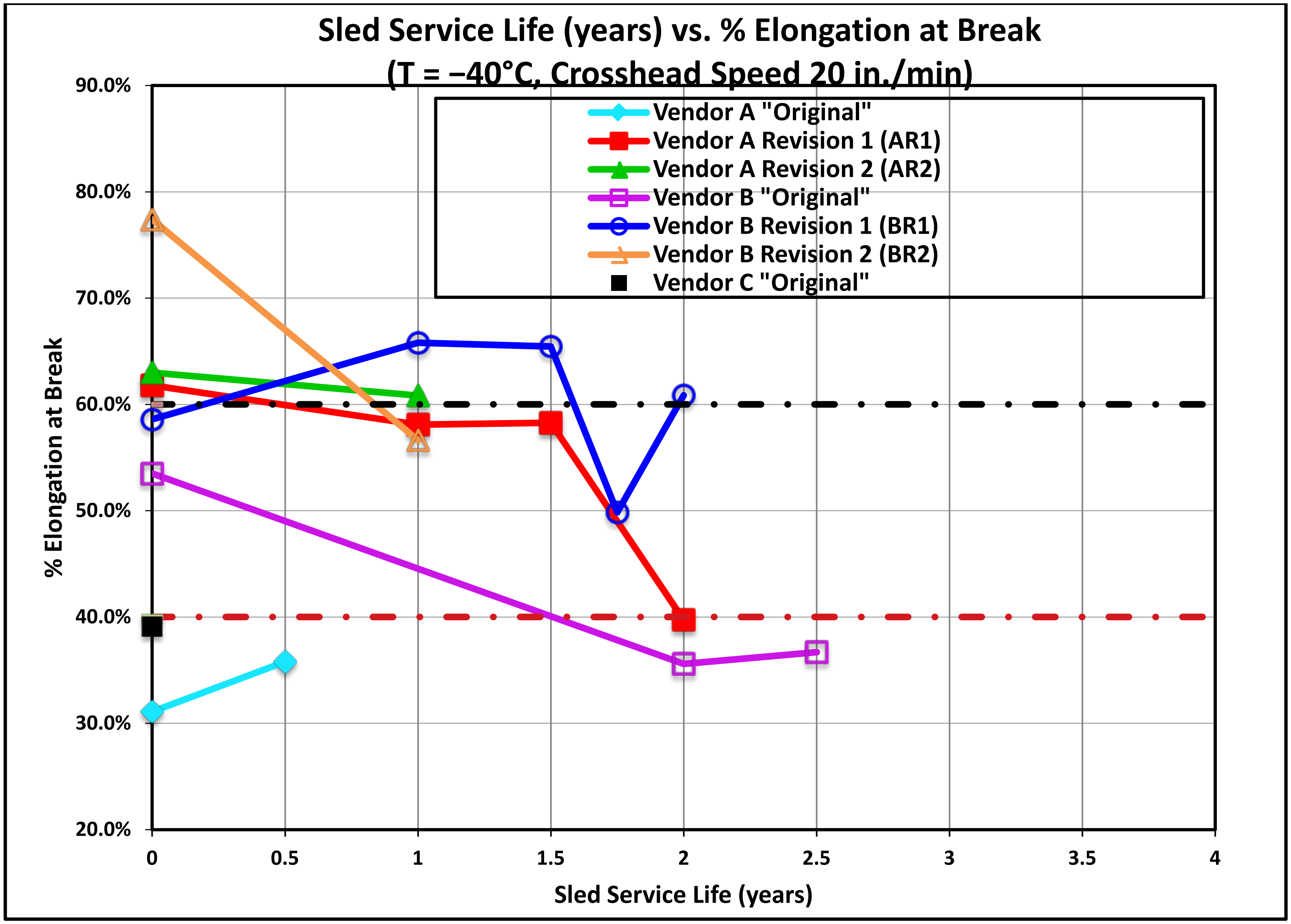

10 Discussion and Recommendations

Despite the high towing efficiency of fuel-bladder sleds, SPoT and GrIT cannot tolerate high rates of in-service HMW-PE failures. SPoT08-09 saw 26% of its original white HMW-PE sheets fail during their first year in service, and this increased to a whopping 71% during SPoT09-10. The viability of fuel-bladder sleds, and thus the economic viability of SPoT, was endangered by these failures and the consequent schedule delays and risks of fuel spills. However, SPoT09-10 bladder sleds also included a set of four original Vendor B black sheets, and these sheets experienced no failures. This offered hope for alternate, acceptable sled material. Unfortunately, SPoT's attempt to acquire more black HMW-PE sheets resulted in Vendor A's original sheets being placed into service, and these failed in large numbers during their first two years (13% on SPoT10-11 and 60% on SPoT11-12). GrIT11 also saw 50% of its black HMW-PE sheets from Vendor C fail early during their first year of service. Clearly, both traverses required performance specifications for HMW-PE acquisitions that would allow them to select the best available material for their polar sleds.

The tensile-test program described here has provided the required specifications. Because the failures were unrelated to towing stresses but showed signs of low ductility, we sought HMW-PE material with the greatest practical low-temperature, high deformation-rate ductility. We conducted an initial series of tensile tests on the original COTS formulations by following ASTM D638, *Standard Test Method for Tensile Properties of Plastics* (ASTM 2010), and selected a temperature of −40°C and a crosshead rate of 20 in./min as our standard test conditions. The resulting values of EAB were very consistent for each HMW-PE formulation and became our measure for low-temperature ductility. This initial series identified Vendor B's original material as having the greatest EAB of the COTS formulations tested (53.3%), and the four bladder sleds that used this material survived two full seasons on SPoT intact. We thus established 50% as a specification for minimum EAB as tested through ASTM (2010) D638 tensile tests conducted at −40°C and at a crosshead rate of 20 in./min. Table 9 provides the set of material specifications used by SPoT and GrIT for subsequent HMW-PE sheet procurements.

Table 9. 2011 HMW-PE material specifications, as provided to the vendors, for polar sleds. Note the increase in specified elongation at break in 2012.

Property	Value	Comment
Tensile strength at yield	>3000 psi	ASTM D638, 20 in./min, −40°F
Tensile strength at break	>4000 psi	ASTM D638, 20 in./min, −40°F
Elongation at break	>50% (2011) >60% (2012)	ASTM D638, 20 in./min, −40°F
Tensile modulus	<420,000 psi	ASTM D638, 20 in./min, −40°F
Brittleness Temperature	<−180°F	ASTM D746
Carbon black content	>1% by mass	2%–2.5% preferred

We selected the values for tensile strength, tensile modulus, and brittleness temperature based on spec sheets provided by Vendors A and B. We set a minimum and preferred range for carbon black to allow vendors to increase UV tolerance as best they saw fit. Vendor B's original material could meet our minimum EAB of 50%, and we encouraged Vendor A to participate in an effort to increase the low-temperature ductility of its product. The resulting two revisions from both vendors have exceeded this minimum, and the resulting sleds have experienced no in-service failures. For sleds procured in 2012 and later, we increased the specified minimum EAB to 60% to allow for greater loss in ductility with service age and thereby extend the service life of the sleds. SPoT and GrIT continue to use these specifications for HMW-PE procurements.

Figure 21 summarizes the success of our collective efforts to reduce in-service sled failures via revised HMW-PE formulations. The Revision 1 sheets entered service on SPoT11-12 and have now survived three operational seasons on SPoT and two on GrIT with no in-service failures. The newer Revision 2 sheets have similarly performed well.

Figure 21. Progress in decreasing the number of in-service HMW-PE failures. This improvement has resulted from systematic tensile testing, cooperative involvement of vendors, and setting specifications for initial elongation at break.

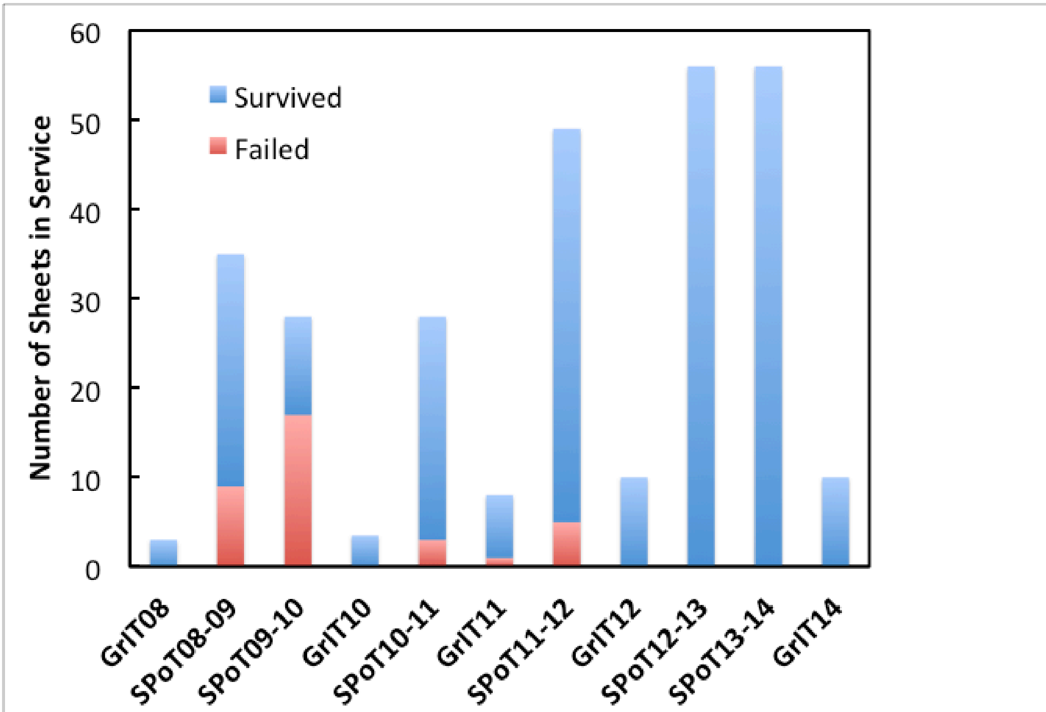

The revised HMW-PE formulations show promise to extend practical service life of Polar sleds from 1 to 2 years to an acceptable range of 5 to 7 years. Moreover, continued tensile testing offers a way to predict the service life of each production run of HMW-PE sheets and thereby provide a measure of operational reliability for SPoT and GrIT. These are both significant benefits derived from the tensile-test program described here.

We make the following recommendations to NSF-PLR and its two traverse contractors based on this work:

- Continue to use Table 9 “HMW-PE material specifications” (with EAB > 60%) for HMW-PE procurements for polar sleds.
- Continue to evaluate newly procured HMW-PE material and samples from in-service sleds for EAB based on ASTM D638, *Standard Test Method for Tensile Properties of Plastics* (ASTM 2010), and at −40°C and 20 in./min.
- Continue to track EAB and in-service sheet failures by service age and production run to update the sled service-life plot (Figure 20).

- We expect that in-service sheet failures will occur for the revised HMW-PE formulations once EAB drops below 40%. If experience confirms this expectation, remove sleds from service based on tensile tests conducted prior to the season by using 40% as the acceptable in-service threshold.

References

ASTM. 2010. *Standard Test Method for Tensile Properties of Plastics*. ASTM D638-10. West Conshohocken, PA: ASTM International.

ASTM. 2014. *Standard Test Method for Brittleness Temperature of Plastics and Elastomers by Impact*. ASTM D746-14. West Conshohocken, PA: ASTM International.

Lever, J. H., and J. C. Weale. 2012. High efficiency fuel sleds for polar traverses. *Journal of Terramechanics* 49:207–213.

Lever, J. H., and P. Thur. 2014. *Economic analysis of the South Pole Traverse*. ERDC/CRREL TR-14-7. Hanover, NH: U.S. Army Research Engineering Development Center.

Appendix A: Physical Properties for HMW-PE as Provided by the Vendors

Table A1. Physical properties as provided by Vendor A.

Vendor A HMW-PE Technical Data Sheet			
Physical Properties	**Metric**	**English**	**Comments**
Specific Gravity	0.949 g/cc	0.03428 lb/in.^{3}	ASTM D1505
Environmental Stress Crack Resistance	>600 hour	>600 hour	Condition A; ASTM D1693
Melt Flow	10.00 g/10 min @ load 21.6 kg, 190°C	10.00 g/10 min @ load 47.6 lb, 374°F	ASTM D1238
Mechanical Properties	**Metric**	**English**	**Comments**
Tensile Strength at Yield	24.82 MPa	3600 psi	ASTM D638
Elongation at Break	>600%	>600%	ASTM D638
Flexural Modulus	1.17 GPa	170 ksi	ASTM D790
Thermal Properties	**Metric**	**English**	**Comments**
Vicat Softening Point	125°C	258°F	ASTM D1525
Brittleness Temperature	≤−90°C	≤−131°F	ASTM D746

Table A2. Physical properties as provided by Vendor B.

Vendor B HMW-PE Technical Data Sheet			
Physical Properties	**Metric**	**English**	**Comments**
Density	0.9485 g/cc	0.03427 lb/in.^{3}	ASTM D4883
Environmental Stress Crack Resistance	≥5000 hour	≥5000 hour	Condition C; ASTM D1693
Melt Flow	8.00 g/10 min @ load 21.6 kg, 190°C	8.00 g/10 min @ load 47.6 lb, 374°F	ASTM D1238
Mechanical Properties	**Metric**	**English**	**Comments**
PENT	≥10,000 hour	≥10,000 hour	Notched Tensile; ASTM F1473
Hardness, Shore D	66.0	66.0	ASTM D2240
Tensile Strength at Break	37.9 MPa	5500 psi	2 in./min; ASTM D638
Tensile Strength at Yield	24.99 MPa	3625 psi	2 in/min;
Elongation at Break	≥600%	≥600%	ASTM D638

Vendor B HMW-PE Technical Data Sheet			
Physical Properties	**Metric**	**English**	**Comments**
Flexural Modulus	1.03 GPa	150 ksi	2% Secant-Method 1; ASTM D790
Izod Impact, Notched	4.81 J/cm	9.00 ft-lb/in.	ASTM D256
Hydrostatic Design Basis	6.89 MPa 11.00 MPa	1000 psi 1600 psi	At 60 C; ASTM D2837 Room Temp; ASTM D2837
Thermal Properties	**Metric**	**English**	**Comments**
Vicat Softening Point	126°C	259°F	ASTM D1525
Brittleness Temperature	≤−118°C	≤−180°F	ASTM D746
Decomposition Temperature	≥220°C	≥428°F	Thermal Stability; ASTM D2513/D3350

Table A3. Physical properties as provided by Vendor C.

Vendor C HMW-PE Technical Data Sheet			
Physical Properties	**Metric**	**English**	**Comments**
Density	0.948 g/cc	59.2 lb/ft^3	ASTM D1505
Environmental Stress Crack Resistance	≥600 hour	≥600 hour	Condition A&B; ASTM D1693
Melt Flow (HLMI)	10 g/10 min @ load 21.6 kg, 190°C	10 g/10 min @ load 47.6 lb, 374°F	ASTM D1238
Mechanical Properties	**Metric**	**English**	**Comments**
Hardness, Shore D	68.0	68.0	ASTM D2240
Tensile Impact Strength	190 KJ/m^2	90 ft-lb/in.^{2}	ASTM D1822
Tensile Strength at Yield	24.8 MPa	3600 psi	ASTM D638
Elongation at Break	≥700%	≥700%	ASTM D638
Flexural Modulus	1207 MPa	175 ksi	2% Secant-Method 1; ASTM D790
Thermal Properties	**Metric**	**English**	**Comments**
Vicat Softening Point	126°C	258°F	ASTM D1525
Brittleness Temperature	≤−75 °C	≤−103°F	ASTM D746
Heat Deflection Temperature @ 66 psi	78°C	173°F	ASTM D648

Appendix B: New, Unused, and Field Sample Dimensions

Table B1. Vendor A new, unused and field sample dimensions*

Sample #		Width (in.)	Thickness (in.)	Area (in.²)	Sample #		Width (in.)	Thickness (in.)	Area (in.²)
A-1		0.754	0.492		A-13		0.749	0.498	
		0.753	0.493				0.744	0.497	
		0.755	0.495				0.745	0.493	
	avg	0.754	0.493	0.372		avg	0.746	0.496	0.370
A-2		0.754	0.491		A-14		0.751	0.494	
		0.753	0.493				0.750	0.494	
		0.759	0.495				0.748	0.495	
	avg	0.755	0.493	0.372		avg	0.750	0.494	0.371
A-3		0.752	0.495		A-15		0.748	0.494	
		0.750	0.494				0.750	0.494	
		0.752	0.493				0.748	0.492	
	avg	0.751	0.494	0.371		avg	0.749	0.493	0.369
A-4		0.745	0.493		A-16		0.754	0.493	
		0.745	0.494				0.756	0.496	
		0.746	0.495				0.755	0.496	
	avg	0.745	0.494	0.368		avg	0.755	0.495	0.374
A-5		0.748	0.497		A-17		0.749	0.496	
		0.754	0.496				0.749	0.495	
		0.749	0.497				0.749	0.495	
	avg	0.750	0.497	0.373		avg	0.749	0.495	0.371
A-6		0.753	0.498		A-18		0.742	0.494	
		0.757	0.497				0.743	0.496	
		0.758	0.494				0.742	0.495	
	avg	0.756	0.496	0.375		avg	0.742	0.495	0.367
A-7		0.747	0.500		A-19		0.747	0.494	
		0.752	0.499				0.750	0.495	
		0.749	0.500				0.749	0.495	
	avg	0.749	0.500	0.374		avg	0.749	0.495	0.370

* "A" series and Antarctic field sample dimensions ("AFS" series).

Sample #		Width (in.)	Thickness (in.)	Area (in.²)	Sample #		Width (in.)	Thickness (in.)	Area (in.²)
A-8		0.752	0.498		A-20		0.742	0.491	
		0.754	0.497				0.743	0.488	
		0.753	0.495				0.744	0.485	
	avg	0.753	0.497	0.374		avg	0.743	0.488	0.363
A-9		0.756	0.494		A-21		0.756	0.492	
		0.755	0.497				0.754	0.495	
		0.755	0.500				0.753	0.496	
	avg	0.755	0.497	0.375		avg	0.754	0.494	0.373
A-10		0.750	0.499		A-22		0.743	0.492	
		0.751	0.497				0.742	0.494	
		0.747	0.500				0.743	0.494	
	avg	0.749	0.499	0.374		avg	0.743	0.493	0.366
A-11		0.748	0.499		A-23		0.748	0.487	
		0.750	0.496				0.742	0.486	
		0.749	0.498				0.742	0.490	
	avg	0.749	0.498	0.373		avg	0.744	0.488	0.363
A-12		0.748	0.499		A-24		0.750	0.494	
		0.745	0.497				0.747	0.489	
		0.746	0.496				0.746	0.489	
	avg	0.746	0.497	0.371		avg	0.748	0.491	0.367

Sample #		Width (in.)	Thickness (in.)	Area (in.²)	Sample #		Width (in.)	Thickness (in.)	Area (in.²)
AFS-1		0.766	0.494		AFS-4		0.754	0.493	
		0.764	0.493				0.754	0.494	
		0.765	0.494				0.753	0.494	
	avg	0.765	0.494	0.378		avg	0.754	0.494	0.372
AFS-2		0.752	0.494		AFS-5		0.751	0.492	
		0.753	0.494				0.751	0.492	
		0.752	0.494				0.752	0.493	
	avg	0.752	0.494	0.372		avg	0.751	0.492	0.370
AFS-3		0.752	0.499		AFS-6		0.750	0.493	
		0.751	0.499				0.746	0.492	
		0.751	0.499				0.751	0.491	
	avg	0.751	0.499	0.375		avg	0.749	0.492	0.369

Table B2. Vendor B new, unused and field sample dimensions*

Sample #		Width (in.)	Thickness (in.)	Area (in.²)	Sample #		Width (in.)	Thickness (in.)	Area (in.²)
B-1		0.747	0.487		B-13		0.746	0.479	
		0.745	0.488				0.744	0.483	
		0.745	0.484				0.741	0.481	
	avg	0.746	0.486	0.363		avg	0.744	0.481	0.358
B-2		0.752	0.485		B-14		0.749	0.477	
		0.752	0.489				0.750	0.477	
		0.752	0.487				0.750	0.476	
	avg	0.752	0.487	0.366		avg	0.750	0.477	0.357
B-3		0.752	0.480		B-15		0.748	0.478	
		0.753	0.484				0.750	0.477	
		0.755	0.485				0.749	0.477	
	avg	0.753	0.483	0.364		avg	0.749	0.477	0.358
B-4		0.754	0.486		B-16		0.749	0.475	
		0.754	0.485				0.748	0.480	
		0.752	0.484				0.749	0.477	
	avg	0.753	0.485	0.365		avg	0.749	0.477	0.357
B-5		0.749	0.483		B-17		0.742	0.470	
		0.750	0.487				0.743	0.474	
		0.747	0.487				0.742	0.472	
	avg	0.749	0.486	0.364		avg	0.742	0.472	0.350
B-6		0.752	0.484		B-18		0.748	0.481	
		0.750	0.485				0.748	0.481	
		0.750	0.484				0.747	0.480	
	avg	0.751	0.484	0.364		avg	0.748	0.481	0.359
B-7		0.749	0.484		B-19		0.747	0.477	
		0.748	0.487				0.748	0.476	
		0.744	0.484				0.748	0.476	
	avg	0.747	0.485	0.362		avg	0.748	0.476	0.356
B-8		0.747	0.482		B-20		0.745	0.482	
		0.748	0.485				0.744	0.479	
		0.748	0.483				0.740	0.477	
	avg	0.748	0.483	0.361		avg	0.743	0.479	0.356

* "B" series and Antarctic field sample dimensions ("BFS" series).

Sample #		Width (in.)	Thickness (in.)	Area (in.²)	Sample #		Width (in.)	Thickness (in.)	Area (in.²)
B-9		0.750	0.488		B-21		0.751	0.481	
		0.753	0.488				0.751	0.480	
		0.754	0.488				0.747	0.476	
	avg	0.752	0.488	0.367		avg	0.750	0.479	0.359
B-10		0.750	0.475		B-22		0.742	0.479	
		0.749	0.476				0.745	0.479	
		0.750	0.477				0.743	0.479	
	avg	0.750	0.476	0.357		avg	0.743	0.479	0.356
B-11		0.743	0.476		B-23		0.742	0.476	
		0.742	0.480				0.744	0.481	
		0.742	0.479				0.742	0.478	
	avg	0.742	0.478	0.355		avg	0.743	0.478	0.355
B-12		0.749	0.479		B-24		0.751	0.479	
		0.750	0.478				0.749	0.478	
		0.749	0.497				0.747	0.476	
	avg	0.749	0.485	0.363		avg	0.749	0.478	0.358
					B-25		0.749	0.483	
							0.750	0.481	
							0.749	0.484	
						avg	0.749	0.483	0.362

Sample #		Width (in.)	Thickness (in.)	Area (in.²)	Sample #		Width (in.)	Thickness (in.)	Area (in.²)
BFS-1		0.751	0.484		BFS-4		0.753	0.485	
		0.751	0.487				0.752	0.486	
		0.749	0.487				0.752	0.486	
	avg	0.750	0.486	0.365		avg	0.752	0.486	0.365
BFS-2		0.751	0.485		BFS-5		0.751	0.486	
		0.752	0.486				0.751	0.487	
		0.751	0.489				0.751	0.487	
	avg	0.751	0.487	0.366		avg	0.751	0.487	0.365
BFS-3		0.751	0.487		BFS-6		0.753	0.487	
		0.752	0.486				0.752	0.488	
		0.752	0.487				0.752	0.489	
	avg	0.752	0.487	0.366		avg	0.752	0.488	0.367

Appendix C: Crosshead Rate Calculation

Estimated Maximum Strain Rate in HMW-PE Sled

Assumptions

1. Sastrugi have circular crests, and maximum strain occurs over a quarter circular arc.
2. A minimum crest radius of r = 10 in.
3. The distance from the center of a sheet to the point of maximum strain = c.

Strain Calculation

1. Maximum strain in a 0.5 in. thick (t) sheet occurs at 0.5t = 0.25 in.
2. Percent strain = $\frac{c}{r} = \frac{0.25\text{ in.}}{10\text{ in.}}$ =0.025 or 2.5%.
3. Sled velocity = 2 m/s = 78.74 in./s.
4. For a quarter circle, arc length $= \frac{\pi r}{2} = \frac{\pi 10\text{ in.}}{2} = 15.71$ in.
5. Assuming the sled experiences maximum strain at half of the arc length, $d = \frac{15.71 in}{78.74}$ = 7.85 in.
6. Thus $\frac{\text{d}}{\text{v}}$ gives a time to maximum strain of $\frac{7.85\text{ in.}}{78.74\text{ in./s}}$ ≈ 10 s.
7. Strain rate = $\frac{\%\text{ strain}}{\text{time to d}} = \frac{0.025\%}{0.10\text{ s}} = \frac{0.25}{\text{s}}$ ≈ 25%.

Crosshead speed calculation

1. 25% = $\frac{0.25}{s} = \frac{0.25}{s} * \frac{60s}{min} = \frac{15.00}{min}$.
2. Crosshead speed = strain rate × gage length = $\frac{15.00}{min} * 2.25\text{ in.} = \frac{33.75\text{ in.}}{min}$. ≈ 34 in./min.

Therefore, begin with the ASTM (2010) spec of 20 in./min and move up to 40 in./min and above.

Appendix D: Summary of Results for Individual Vendor Samples

Table D1. Summary of results for individual Vendor A samples.

Test Series		Sample #	Max. Stress (psi)	Failure Stress (psi)	Failure Displacement (in.)	Young's Modulus (psi)	Color Key
A.1		A-21				174582	File Problem
		A-21a	4263.775	2149.9	2.19		See plots
		A-22	4329.78	2099.599	2.153	175874	Slipped
		A-23	4333.25	2088.606	2.139	181875	Did not break
		A-24	4334.12	2220.509	2.141	178766	Pin not removed
	avg.		4315.23125	2139.6535	2.15575	177774.25	Sample Broke Immediately
	st. dev.		34.3553587	60.1465235	0.02365551	3245.567683	
A.2		A-1	6202.6	3374.5	0.858		
		A-2	6278.56	3257.22	0.909	335103	
		A-3				327561	
		A-3a					
		A-3b	6267.893	3047.18	0.994		
		A-4	6323.43	3304.37	0.936	323948	
		A-5	6246.13	3262.64	0.901	327547	
	avg.		6263.7226	3249.182	0.9196	328539.75	
	st. dev.		44.2944299	122.2710633	0.0501428	4694.107041	
A.3		A-6				425362	
		A-6a	7730.35	3970.3	0.685		
		A-7	7410.76	3909.63	0.677	449867	
		A-8	7360.52	3667.08	0.717	390278	
		A-9				393679	
		A-9a	7303.74	3757.58	0.761		
		A-10	7405.39	3768.9	0.66	393945	
	avg.		7442.152	3814.698	0.7	410626.2	
	st. dev.		166.745806	122.8566885	0.03988734	26155.79979	
A.4		A-11	7532.45	4137.4	0.644	410102	
		A-12				398705	
		A-12a	7535.49	4113.37	0.733		
		A-13				408962	
		A-13a	7578.16	4352.82	0.589		
		A-14	7497.02	3864.4	0.809	401114	
		A-15				413474	

Test Series		Sample #	Max. Stress (psi)	Failure Stress (psi)	Failure Displacement (in.)	Young's Modulus (psi)	Color Key
		A-15a					File Problem
		A-15b	7610.81	3853.77	0.866		See plots
	avg.		7550.786	4064.352	0.7282	406471.4	Slipped
	st. dev.		44.196085	209.3311627	0.114025	6273.744002	Did not break
A.5		A-16	7565.99	3777.37	0.784	405477	Pin not removed
		A-17	7660.28	4103.15	0.695	397460	Sample Broke Immediately
		A-18	7663.85	4163.24	0.766	405510	
		A-19				401317	
		A-19a	7644.82	4076.32	0.802		
		A-20	7818.6	3877.04	0.691	418460	
	avg.		7670.708	3999.424	0.7476	405644.8	
	st. dev.		91.7385784	164.1596647	0.05146164	7905.638538	
AFS.1		AFS-1	7183.25	3440.01	0.834	392776	
		AFS-2	7233.168	2959.106	0.808	395897	
		AFS-3	7233.357	3426.27	0.805	388467	
		AFS-4	7240.729	3688.497	0.808	376134	
		AFS-5	7305.572	3666.732	0.775	396001	
		AFS-6	7247.31			399165	
	avg.		7239.2152	3436.123	0.806	389855	
	st. dev.		43.6133788	293.4836262	0.02094039	8261.411895	

Table D2. Summary of results for individual Vendor B samples.

Test Series		Sample #	Maximum Stress (psi)	Failure Stress (psi)	Failure Displacement (in.)	Young's Modulus (psi)	Color Key
B.1		B-21	4188.403	2485.78	4.13	186442	File Problem
		B-22	4213.81	2680.835	3.815	180865	See plots
		B-23	4240.22			190575	Slipped
		B-24	4197.19	2617.651	3.498	186842	Did not break
		B-25	4175.74	2633.934	5.555	186274	Pin not removed
	avg.		4203.0726	2604.55	4.2495	186199.6	Sample Broke Immediately
	st. dev.		24.96044	83.58781766	0.90777255	3466.953028	
B.2		B-1	6137.648	3321.14	1.537	339494	
		B-2				334501	
		B-2a	6154.16	3632.54	1.682		
		B-3	6130.62	3449.415	1.858	341955	
		B-4	6143.11	3645.91	1.669	342373	
		B-5	6175.35	3459.26	1.499	326967	

Test Series		Sample #	Maximum Stress (psi)	Failure Stress (psi)	Failure Displacement (in.)	Young's Modulus (psi)	Color Key
	avg.		6148.1776	3501.653	1.649	337058	File Problem
	st. dev.		17.4567379	136.9784719	0.14161038	6452.334074	See plots
B.3		B-6	7356.31	4228.56	1.132	405540	Slipped
		B-7	7324.4	3997.48	1.32	407390	Did not break
		B-8	7386.27	4181.43	1.128	390133	Pin not removed
		B-9	7264.23	4122.87	1.234	407905	Sample Broke Immediately
		B-10	7445.43	3936.17	1.204	397380	
	avg.		7355.328	4093.302	1.2036	401669.6	
	st. dev.		67.6980961	123.2962476	0.07955376	7714.871891	
B.4		B-11	7577.77	4008.93	1.067	432468	
		B-12	7441.79	3919.78	1.087	459466	
		B-13				451533	
		B-13a	7551.03	4278.02	1.183		
		B-14	7484.9	4324.33	1.128	426175	
		B-15	7529.13	4050.88	1.02	425718	
	avg.		7516.924	4116.388	1.097	439072	
	st. dev.		54.0488111	175.9673296	0.06181828	15487.62811	
B.5		B-16	7641.69	3930.2	1.124	418063	
		B-17	7699.83	3769.87	1.055	427671	
		B-18	7568.18	3872.99	1.12	405924	
		B-19				422704	
		B-19a	7658.62	4478.57	1.247		
		B-20				429676	
		B-20a	7718.26	4309.24	0.99		
	avg.		7657.316	4072.174	1.1072	420807.6	
	st. dev.		58.5506407	305.1952605	0.09546046	9465.800141	
BFS.1		BFS-1	7288.93	3328.45	0.839	400404	
		BFS-2	7247.80	3535.95	0.886	407679	
		BFS-3	7228.16	3633.65	0.814	413741	
		BFS-4	7308.24	2953.18	0.896	414255	
		BFS-5	7353.63	890.57	0.623	425244	
		BFS-6	7222.65	3080.43	0.746	427633	
	avg.		7274.902	2903.705	0.801	414826	
	st. dev.		51.2967341	1019.74199	0.103	10326.0	

Appendix E: Representative Curves for Tensile Test of Field Specimens

Figure E1. Force vs. piston displacement for Vendor A sample AFS-1. Piston-controlled load-displacement plot at −40°C and 20 in./min crosshead speed.

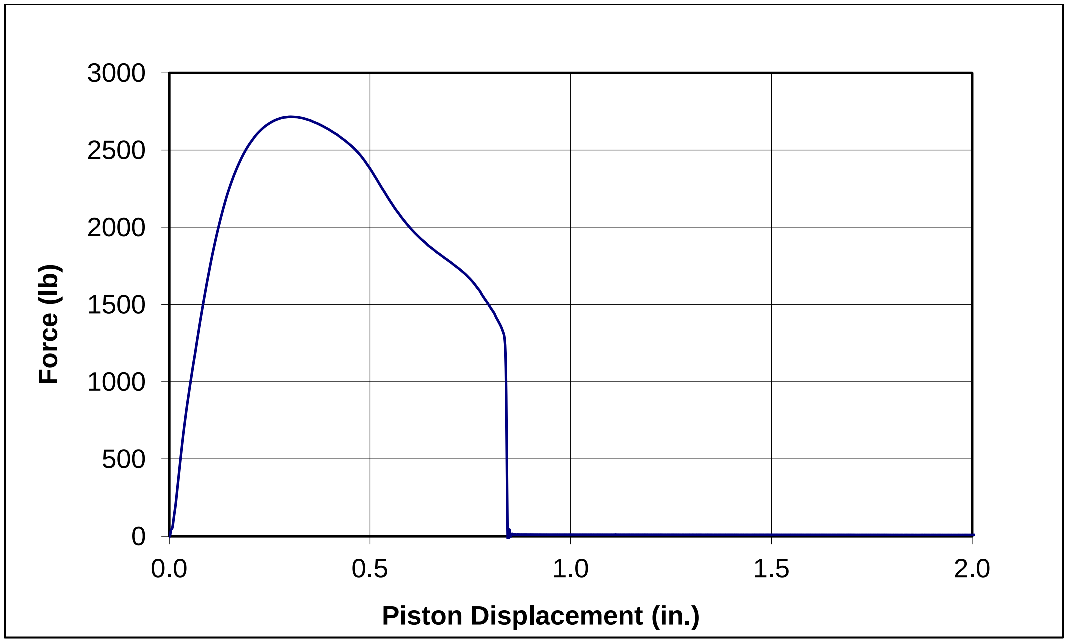

Figure E2. Stress-strain plot for Vendor A sample AFS-1. Piston controlled at −40°C and 20 in./min crosshead speed illustrating Young's modulus calculation.

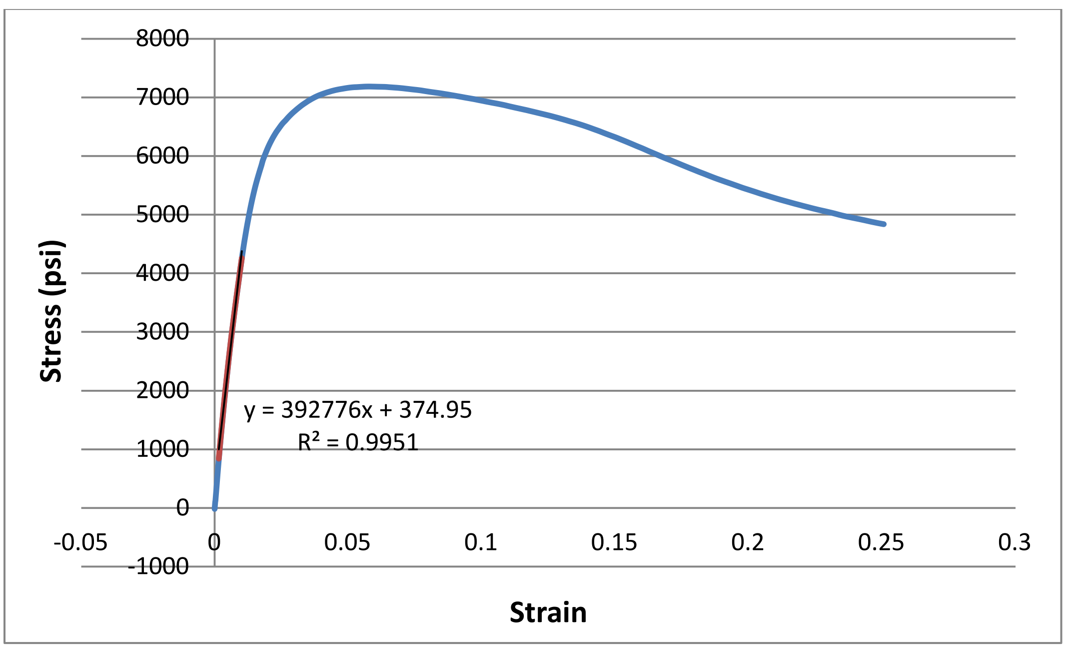

Figure E3. Force vs. piston displacement for Vendor B sample BFS-1. Piston-controlled load-displacement plot at −40°C and 20 in./min crosshead speed.

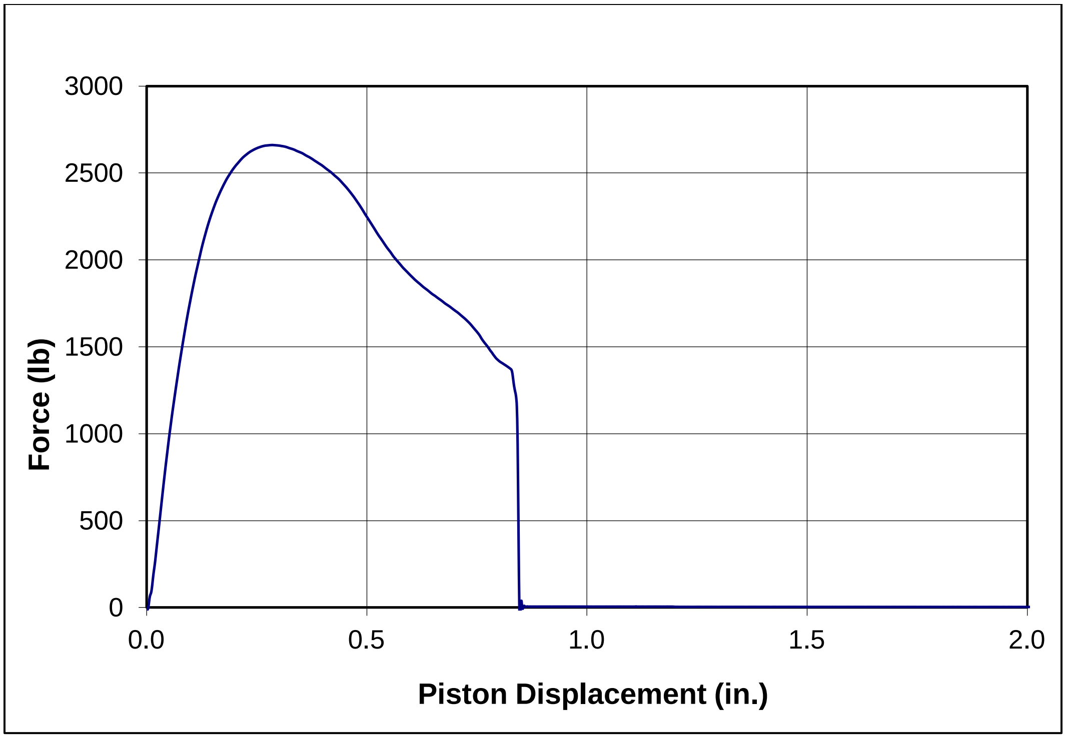

Figure E4. Stress-strain plot for Vendor B sample BFS-1. Piston controlled at −40°C and 20 in./min crosshead speed illustrating Young's modulus calculation.

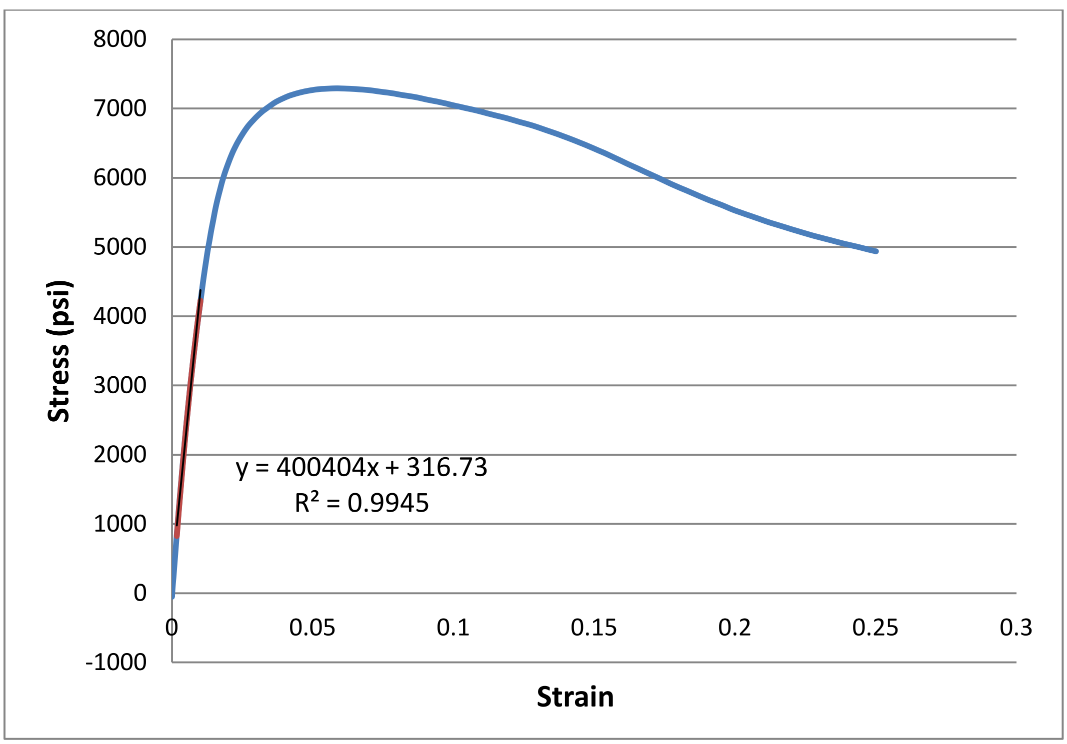

REPORT DOCUMENTATION PAGE

Form Approved
OMB No. 0704-0188

1. REPORT DATE *(DD-MM-YYYY)*
June 2015

2. REPORT TYPE
Technical Report/Final

3. DATES COVERED *(From - To)*

4. TITLE AND SUBTITLE
High-Performance Plastic Sled Design for Polar Traversing

5a. CONTRACT NUMBER

5b. GRANT NUMBER

5c. PROGRAM ELEMENT NUMBER

6. AUTHOR(S)
Jason C. Weale, James H. Lever, and Jonathan Trovillion

5d. PROJECT NUMBER
EP-ARC-10-12, EP-ARC-12-12

5e. TASK NUMBER
EP-ANT-11-05, EP-ANT-12-16, EP-ANT-13-46

5f. WORK UNIT NUMBER

7. PERFORMING ORGANIZATION NAME(S) AND ADDRESS(ES)
Cold Regions Research and Engineering Laboratory (CRREL)
U.S. Army Engineer Research and Development Center (ERDC)
72 Lyme Road
Hanover, NH 03755-1290

8. PERFORMING ORGANIZATION REPORT NUMBER
ERDC TR-15-2

9. SPONSORING / MONITORING AGENCY NAME(S) AND ADDRESS(ES)
National Science Foundation, Division of Polar Programs
Arlington, VA 22230

10. SPONSOR/MONITOR'S ACRONYM(S)
NSF

11. SPONSOR/MONITOR'S REPORT NUMBER(S)

12. DISTRIBUTION / AVAILABILITY STATEMENT
Approved for public release; distribution is unlimited.

13. SUPPLEMENTARY NOTES
Engineering for Polar Operations, Logistics, and Research (EPOLAR)

14. ABSTRACT
Over-snow resupply traverses in Antarctica and Greenland tow high-efficiency fuel sleds that consist of flexible fuel bladders strapped to flexible sheets of high molecular weight polyethylene (HMW-PE). Despite low towing stresses, initial HMW-PE sheets were prone to cracking and failure within 1 to 2 years of service. This report describes the results of low-temperature, uniaxial tensile tests, following ASTM Standard D638, that we used to set specifications on HMW-PE sheets for polar sleds, aiming to increase service life. Tests of the original HMW-PE formulations showed significant reductions in ductility, as measured by percent elongation at break, at −40°C compared with 23°C. HMW-PE manufacturers subsequently cooperated to supply sheets with greater low-temperature ductility, and the rate of sled breakages decreased dramatically. Performance specifications for new HMW-PE sheets for polar traverses now include a requirement for greater than 60% elongation at break at −40°C, as measured using ASTM 638 uniaxial tensile tests.

15. SUBJECT TERMS

Cold-testing HMW-PE	High-performance plastic sleds	NSF
EPOLAR	HMW-PE polar sleds	Polar sled development
	HMW-PE sled durability	Polar traverses

16. SECURITY CLASSIFICATION OF: a. REPORT	b. ABSTRACT	c. THIS PAGE	17. LIMITATION OF ABSTRACT	18. NUMBER OF PAGES	19a. NAME OF RESPONSIBLE PERSON / 19b. TELEPHONE NUMBER *(include area code)*
Unclassified	Unclassified	Unclassified	SAR	66	